Probing BSM with PVDIS at SoLID: Physics Overview

Sonny Mantry
University of North Georgia (UNG)

Workshop on the Physics Program with High Luminosity Facilities

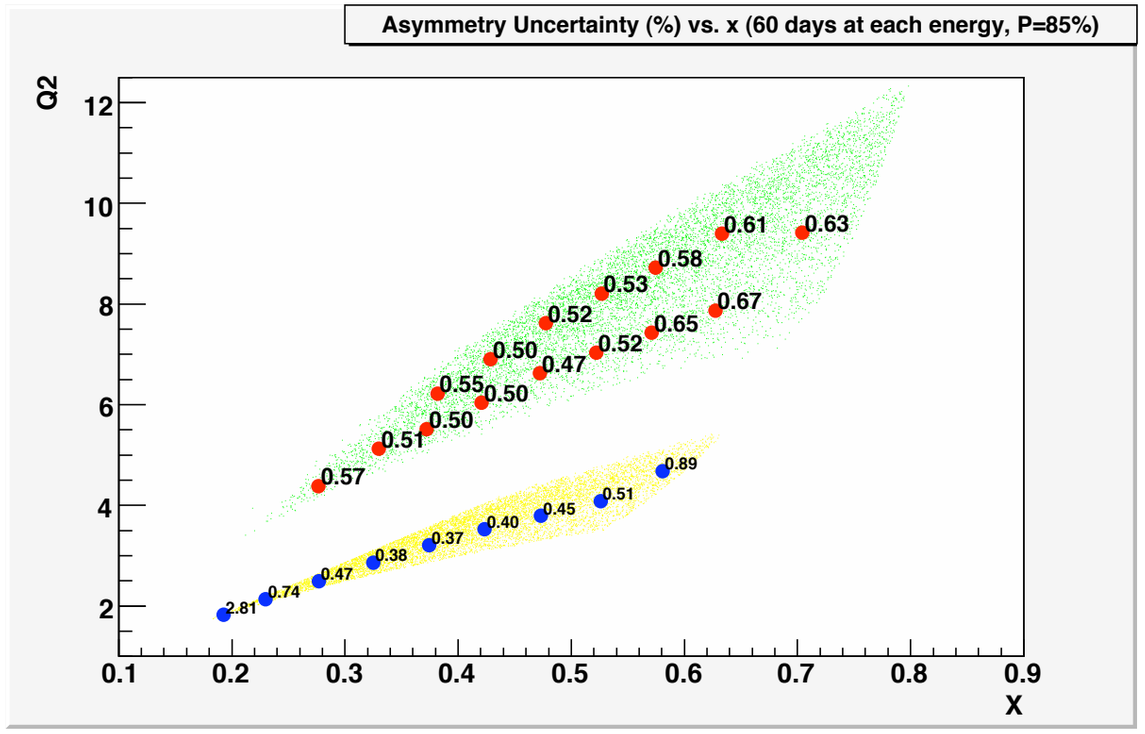
Oct. 5th-9th, 2026

PVDIS at SoLID

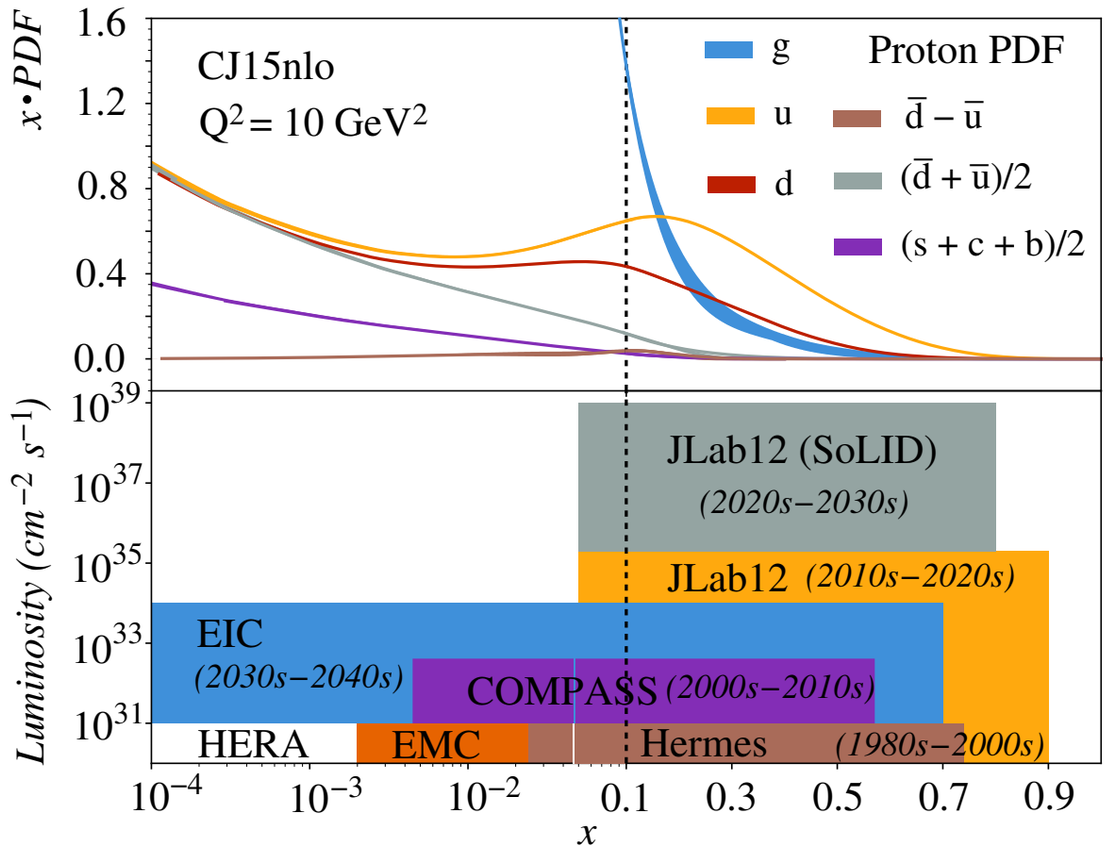
- PVDIS at SoLID:
  - High Luminosity ($\mathscr{L} \sim 10^{39} cm^{-2} s^{-1}$)
  - High data processing rate
  - Kinematics:
    $2\ \mathrm{GeV}^2 \lesssim Q^2 \lesssim 10\ \mathrm{GeV}^2,\ x \gtrsim 0.2$
  - Access to high-x region ($x \gtrsim 0.2$), sea quark effects suppressed
  - Polarized electron beams (85 % polarization)
  - Proton and Deuteron Targets (possibly ^{48}Ca)
  - Deuteron is an isoscalar target, many hadronic effects cancel
  - Extracted physics will be complementary to other low energy experiments (APV,Qweak,MOLLER, P2, etc), the EIC, and the LHC

arXiv:2209.13357, SoLID White Paper

Taken from P. Souder talk



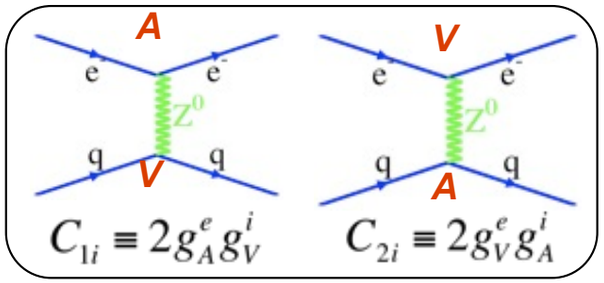
arXiv:2209.13357, SoLID White Paper

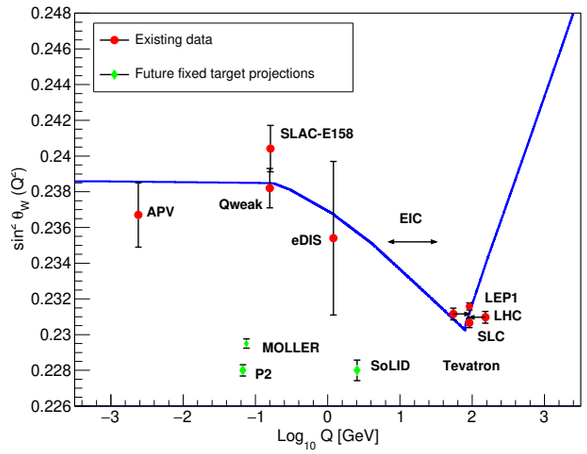


Parity-Violating DIS (PVDIS) at SoLID

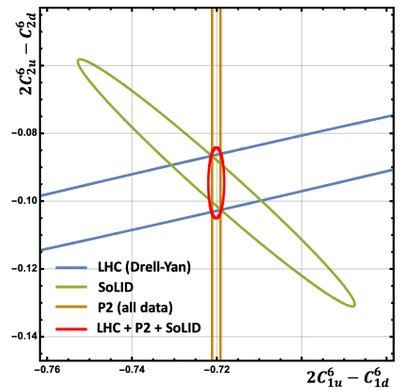
arXiv:2209.13357, SoLID White Paper

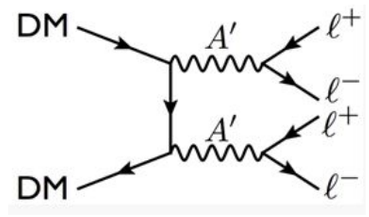
- Precision physics
  - Measure electroweak parameters:
    - C_{iq} couplings
    - Weak Mixing Angle (θ_W)

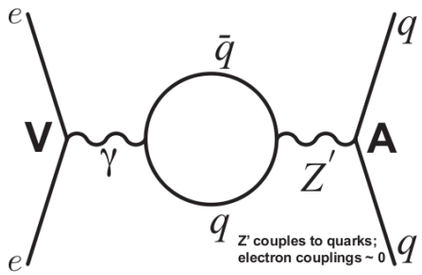


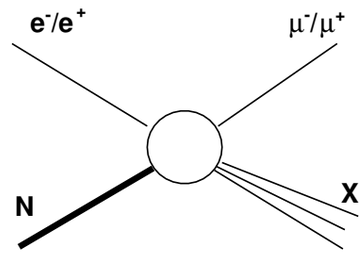


  - Probe BSM physics:
    - BSM reach $\Lambda_{\mathrm{BSM}} \sim 10$ - 20 TeV
    - Leptophobic Z'
    - Dark Photons
    - Dark-Z
    - SMEFT Analysis, lift flat directions
    - Charged Lepton Flavor Violation (CLFV)

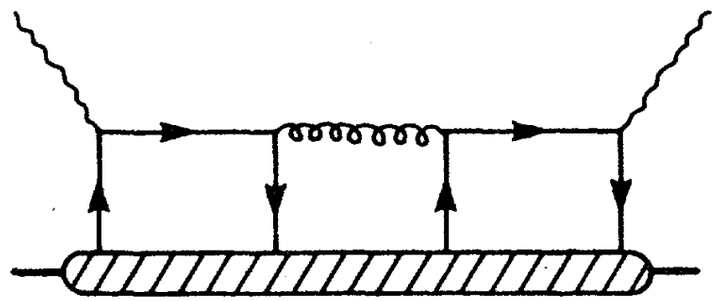




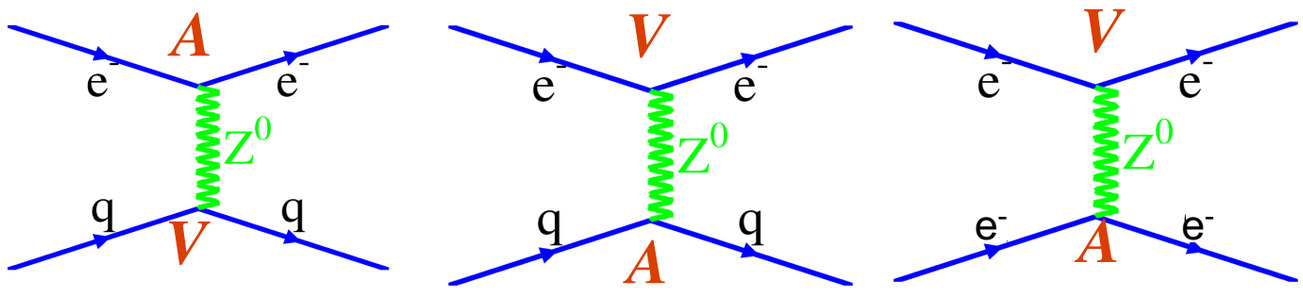




- Hadronic Physics must be under control for clean interpretation:
  - Charge Symmetry Violation (CSV)
  - Higher Twist (HT) Effects
  - d/u proton PDF ratio, free of nuclear effects
  - strange quark PDFs



Contact Interactions



$C_{1i} \equiv 2g_A^e g_V^i$ $C_{2i} \equiv 2g_V^e g_A^i$ $C_{2e} = 2g_V^e g_A^e$

- For $Q^2 << (M_Z)^2$ limit, the effective Lagrangian relevant for PVES scattering is given by:

$$\mathscr{L} = \frac{G_F}{\sqrt{2}} \sum_q \left[C_{1q}\, \bar{e}\gamma^\mu\gamma_5 e\, \bar{q}\gamma_\mu q + C_{2q}\, \bar{e}\gamma^\mu e\, \bar{q}\gamma_\mu\gamma_5 q + C_{2e}\, \bar{e}\gamma^\mu\gamma_5 e\, \bar{e}\gamma_\mu e \right]$$

- Tree-level Standard Model values:

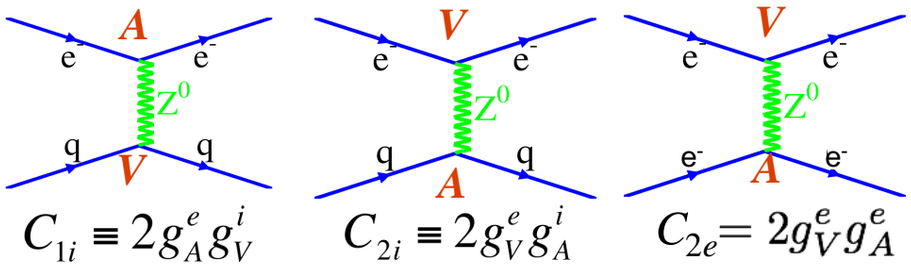
$$C_{1q} = 2g_A^e g_V^q \qquad C_{2q} = 2g_V^e g_A^q \qquad C_{2e} = 2g_A^e g_V^e$$

$$C_{1u} = -\frac{1}{2} + \frac{4}{3}\sin^2\theta_W \qquad C_{2u} = -\frac{1}{2} + 2\sin^2\theta_W$$

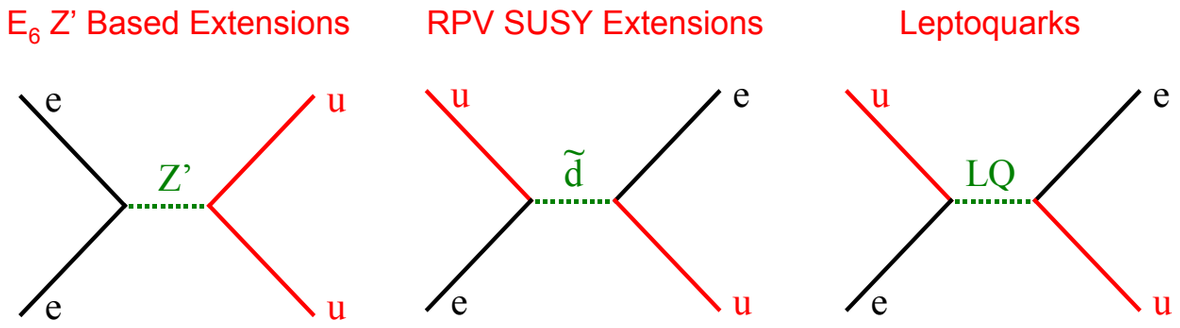
$$C_{1d} = \frac{1}{2} - \frac{2}{3}\sin^2\theta_W \qquad C_{2d} = \frac{1}{2} - 2\sin^2\theta_W$$

$$C_{2e} = \frac{1}{2} - 2\sin^2\theta_W$$

New Physics Effects



+



• In the $Q^2 \ll M_Z^2$ limit, electron-quark interactions via the weak neutral current can be parameterized by contact interactions:

$$\mathscr{L} = \frac{G_F}{\sqrt{2}} \sum_q \left[C_{1q}\, \bar{e}\gamma^\mu\gamma_5 e\, \bar{q}\gamma_\mu q + C_{2q}\, \bar{e}\gamma^\mu e\, \bar{q}\gamma_\mu\gamma_5 q + C_{2e}\, \bar{e}\gamma^\mu\gamma_5 e\, \bar{e}\gamma_\mu e \right]$$

• New physics contact interactions arise as a shift in the WNC couplings compared to the SM prediction:

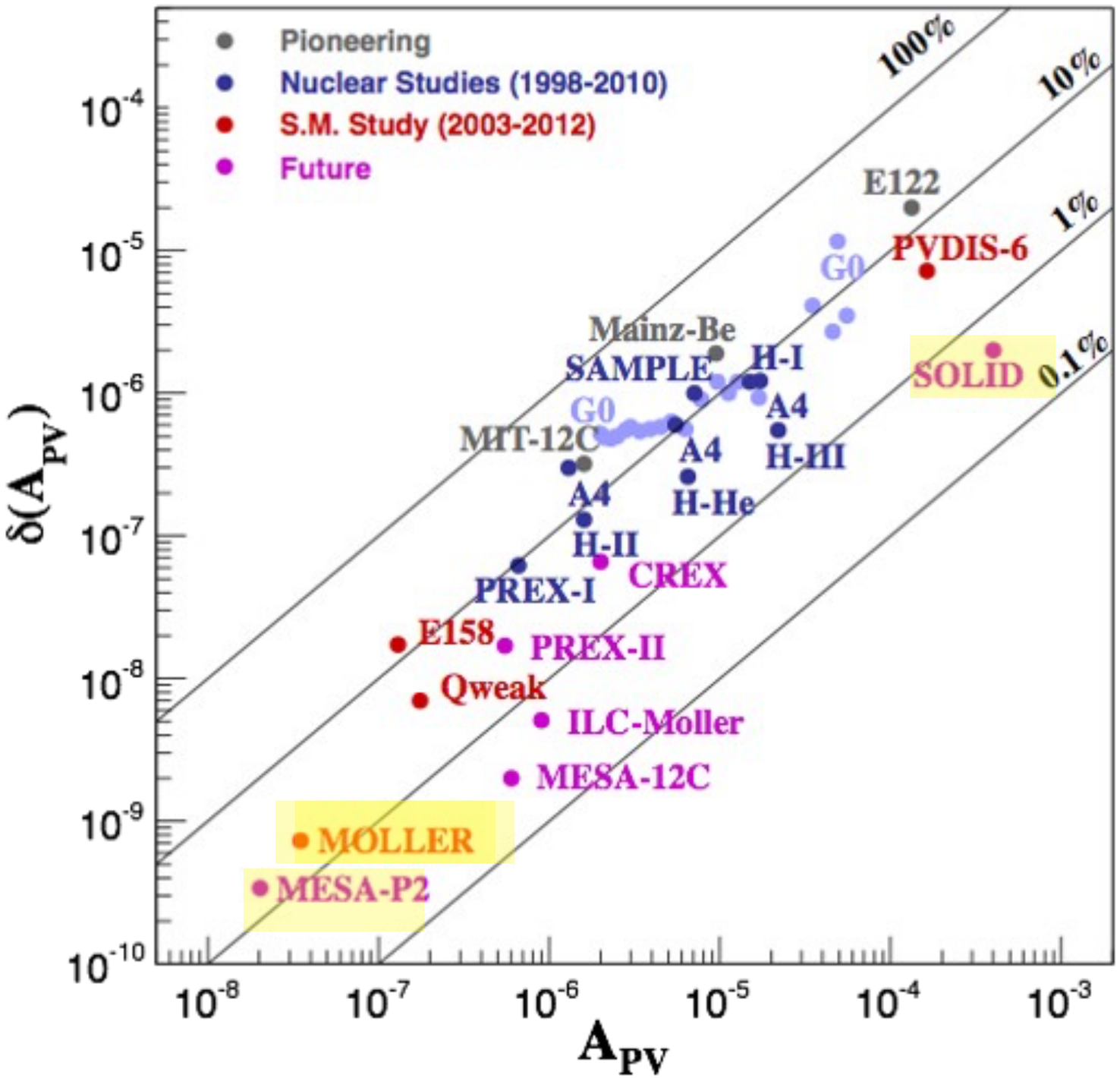
$$C_{iq} = C_{iq}(\mathrm{SM}) + \Delta C_{iq}$$

SM contribution

New Physics contribution

• Deviations from the SM prediction of the WNC couplings will lead to corresponding deviations in the extracted value of the weak mixing angle.

Accessing C_{iq}, C_{2e} via Parity-Violating Observables



	A	δA	δA/A(%)
SoLID	500 ppm	3 ppm	0.6
MOLLER	0.035 ppm	0.0008 ppm	2.2
P2	0.020 ppm	0.0004 ppm	2.0

Taken from P. Souder talk

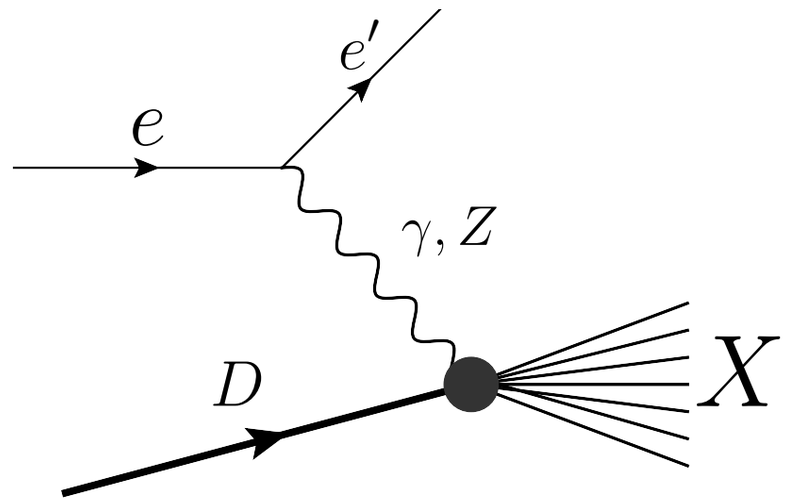
- SoLID, MOLLER, and P2 are all expected to improve precision

- SoLID provides unique opportunities while also being complementary to the wide range of other low energy experiments, the EIC, and the LHC.

Parity-Violating e-D Asymmetry

• Parity-violating e-D asymmetry is a powerful probe of the WNC couplings:

$$A_{\rm PV} \equiv \frac{\sigma_R - \sigma_L}{\sigma_R + \sigma_L} \simeq \frac{|A_Z|}{|A_\gamma|} \simeq \frac{G_F Q^2}{4\pi\alpha} \simeq 10^{-4} \frac{Q^2}{\rm GeV^2}$$



• Due to the isoscalar nature of the Deuteron target, the dependence of the asymmetry on the structure functions largely cancels (Cahn-Gilman formula).

$$A_{\rm CG}^{RL} = -\frac{G_F Q^2}{2\sqrt{2}\pi\alpha}\frac{9}{10}\left[\left(1 - \frac{20}{9}\sin^2\theta_W\right) + \left(1 - 4\sin^2\theta_W\right)\frac{1-(1-y)^2}{1+(1-y)^2}\right]$$

All hadronic effects cancel! → Clean probe of WNC

• e-D asymmetry allows a precision measurement of the weak mixing angle.

Corrections to Cahn-Gilman

- Hadronic effects appear as corrections to the Cahn-Gilman formula:

$$A_{RL} = -\frac{G_F Q^2}{2\sqrt{2}\pi\alpha}\frac{9}{10}\left[\tilde{a}_1 + \tilde{a}_2\frac{1-(1-y)^2}{1+(1-y)^2}\right]$$

$$\tilde{a}_j = -\frac{2}{3}(2C_{ju} - C_{jd})\left[1 + R_j(\text{new}) + R_j(\text{sea}) + R_j(\text{CSV}) + R_j(\text{TMC}) + R_j(\text{HT})\right]$$

New physics

Sea quarks

Charge symmetry violation

Target mass

Higher twist

- Hadronic effects must be well understood before any claim for evidence of new physics can be made.

  [Bjorken, Wolfenstein; Hobbs, Melnitchouk; SM, Ramsey-Musolf, Sacco; Belitsky, Mashanov, Schafer; Seng, Ramsey-Musolf, ….]

- Most recent JAM analysis for SoLID:

  [Whitehill, Dalton, Liu, Melnitchouk, Sato]

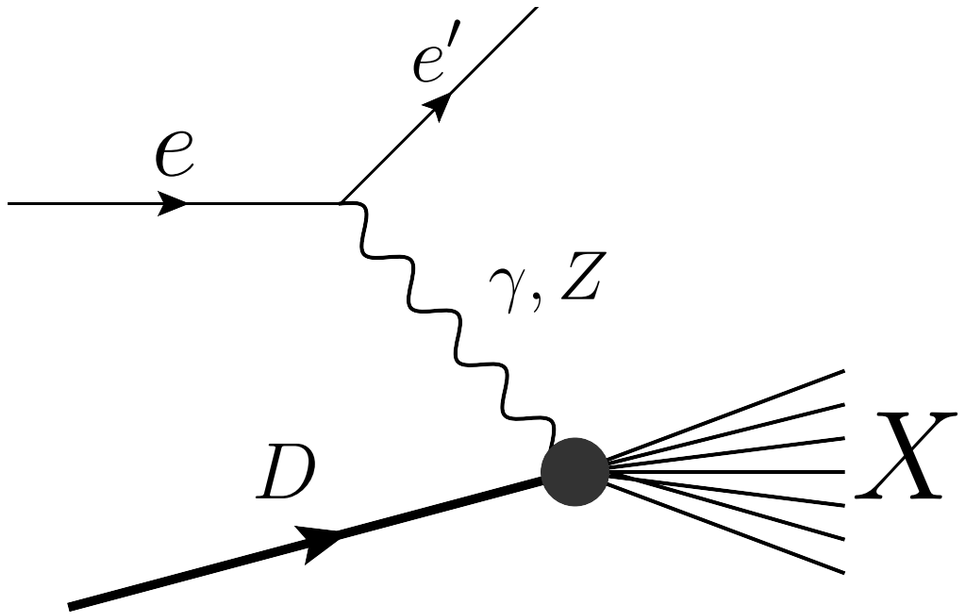
PVDIS Asymmetry

- Parity Violating DIS (E122, PVDIS-6, SOLID):
  Sensitive to C_{1q} and C_{2q}

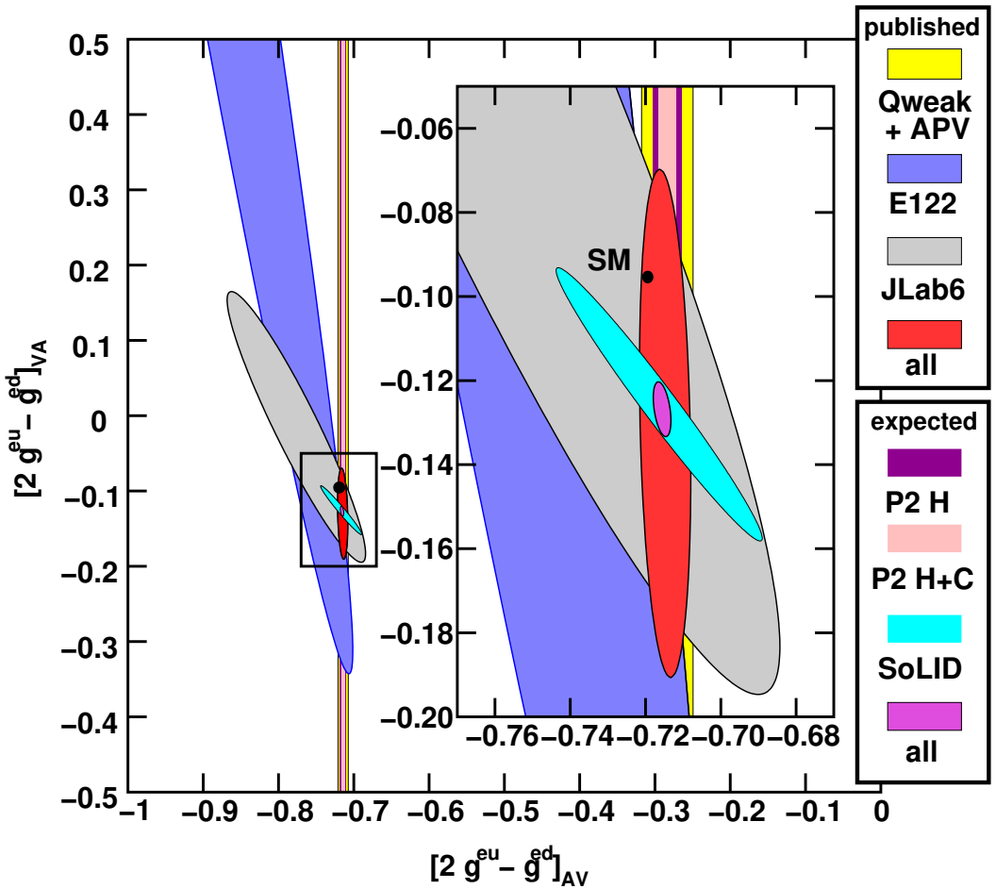
$$A_{\rm PV}^{\rm DIS} = \frac{G_F Q^2}{4\sqrt{2}(1+Q^2/M_Z^2)\pi\alpha}\left[a_1 + \frac{1-(1-y)^2}{1+(1-y)^2}a_3\right]$$

$$a_1 = \frac{2\sum_q e_q C_{1q}(q+\bar{q})}{\sum_q e_q^2 (q+\bar{q})}$$

$$a_3 = \frac{2\sum_q e_q C_{2q}(q-\bar{q})}{\sum_q e_q^2 (q+\bar{q})}$$



Status of C_{1q} and C_{2q} Couplings



- The combination $2C_{1u} - C_{1d}$ is severely constrained by Qweak and Atomic Parity violation.
- The combination $2C_{2u} - C_{2d}$ is known to within ~50% from the JLAB 6 GeV experiment:

$$2C_{2u} - C_{2d} = -0.145 \pm 0.068$$

- First unambiguous non-zero result observed for the C_{2q} couplings!
- SoLID is expected significantly improve on this result for the extraction of the C_{2q} couplings.

PARTICLE PHYSICS

Quarks are not ambidextrous

By separately scattering right- and left-handed electrons off quarks in a deuterium target, researchers have improved, by about a factor of five, on a classic result of mirror-symmetry breaking from 35 years ago. **SEE LETTER P.67**

WILLIAM J. MARCIANO

SoLID Projection Analysis $\sin^2\theta_W$ Extraction

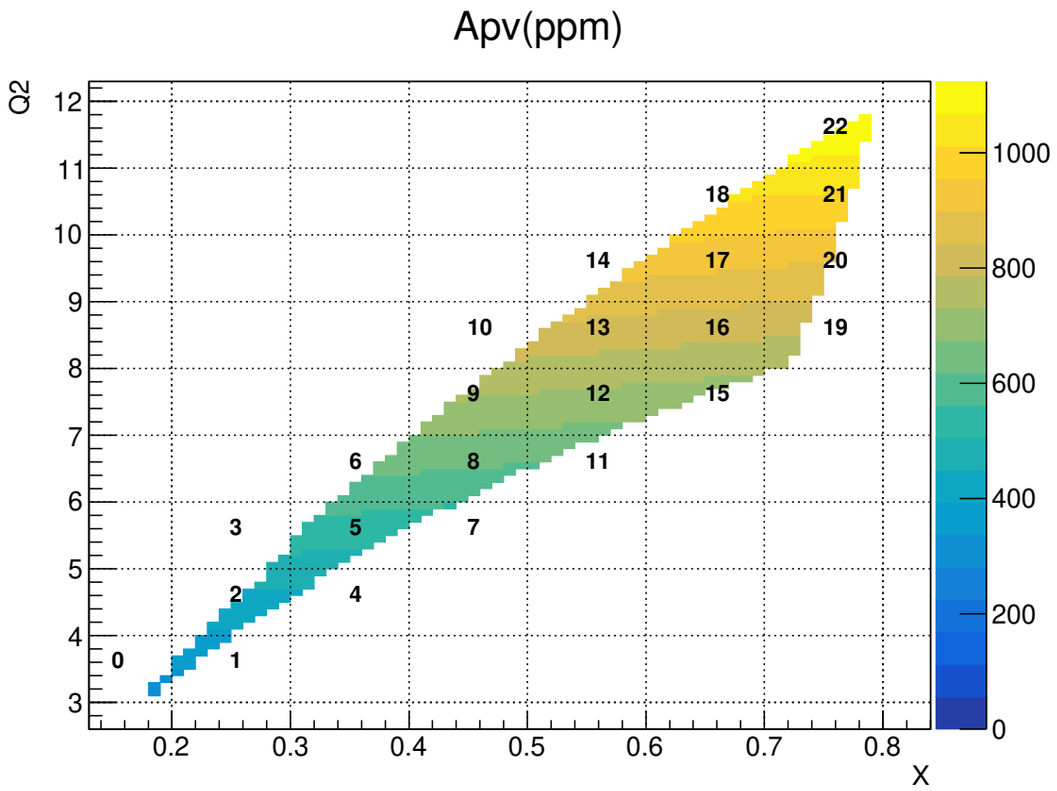


FIG. 11. Illustration of PVDIS asymmetry on a deuteron target in ppm on the (x, Q^2) plane. The data are divided into evenly spaced grid with the bin number shown. The expected statistical uncertainty is less than 1% in most of the bins.

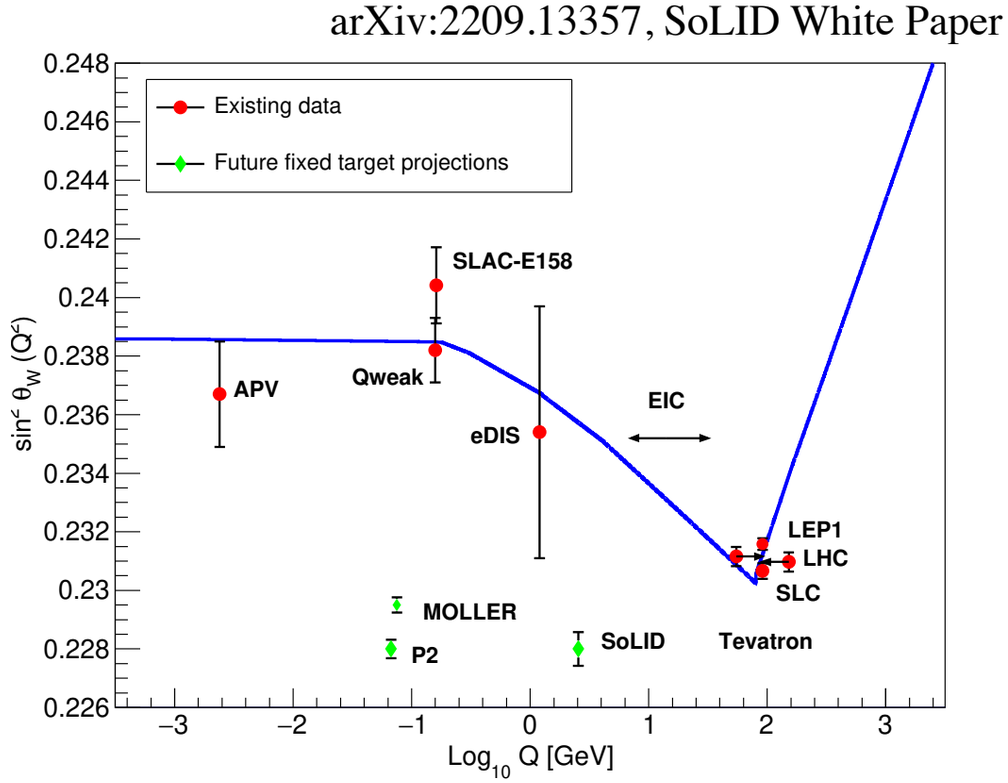


FIG. 12. Experimental determination of the weak mixing angle $\sin^2\theta_W$. Data points for Tevatron and LHC are shifted horizontally for clarity.

$$A_{PV}^{\mathrm{data}} = A_{PV,(d)}^{\mathrm{SM}}\left(1 + \frac{\beta_{\mathrm{HT}}}{(1-x)^3 Q^2} + \beta_{\mathrm{CSV}} x^2\right)$$

Strong Correlation between PDF effects $\sin^2\theta_W$ Extraction

[Whitehill, Dalton, Liu, Melnitchouk, Sato]

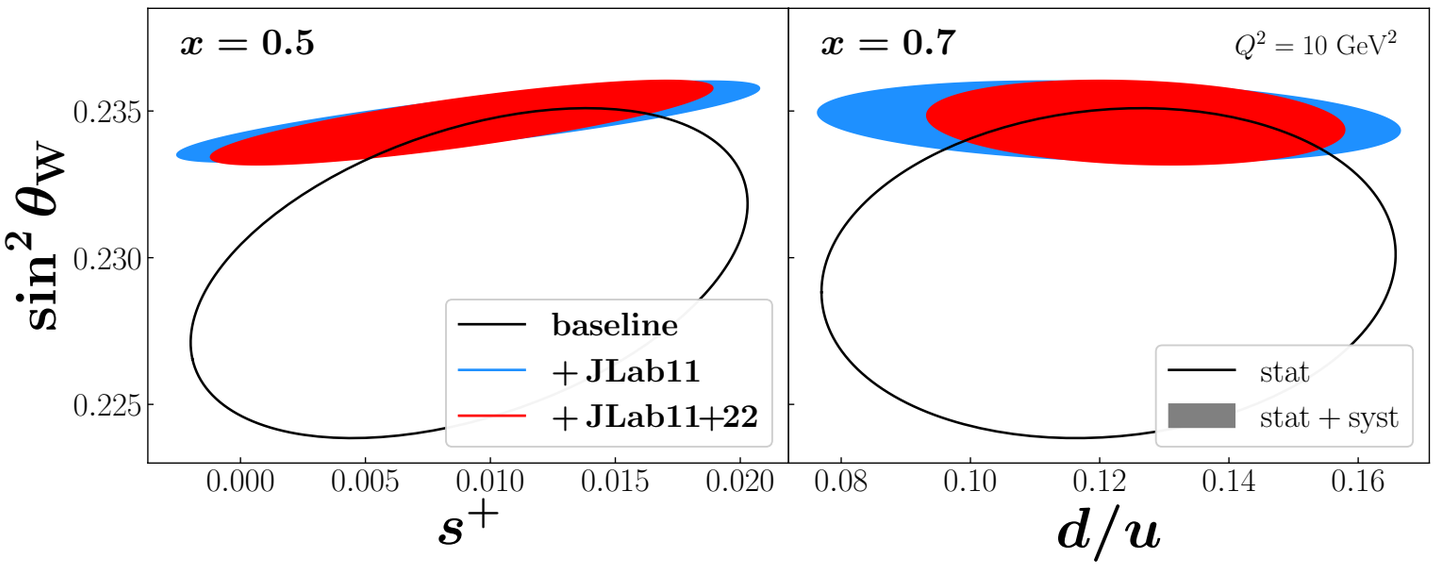


FIG. 10. Joint 68% confidence regions for $\sin^2\theta_W$ with the s^+ PDF at $x = 0.5$ (left) and with the d/u PDF ratio at $x = 0.7$ (right) at $Q^2 = 4$ GeV^2 from a combined fit of PDFs and $\sin^2\theta_W$ using Jefferson Lab 11 GeV pseudodata (blue) and the combined 11 GeV and 22 GeV pseudodata (red), compared with the baseline (black), which is a fit including data from the JAM26 analysis and A_{PV} data from the 6 GeV JLab [65] and SLAC [15, 16].

Combined fits of $\sin^2\theta_W$ and PDFs

[Whitehill, Dalton, Liu, Melnitchouk, Sato]

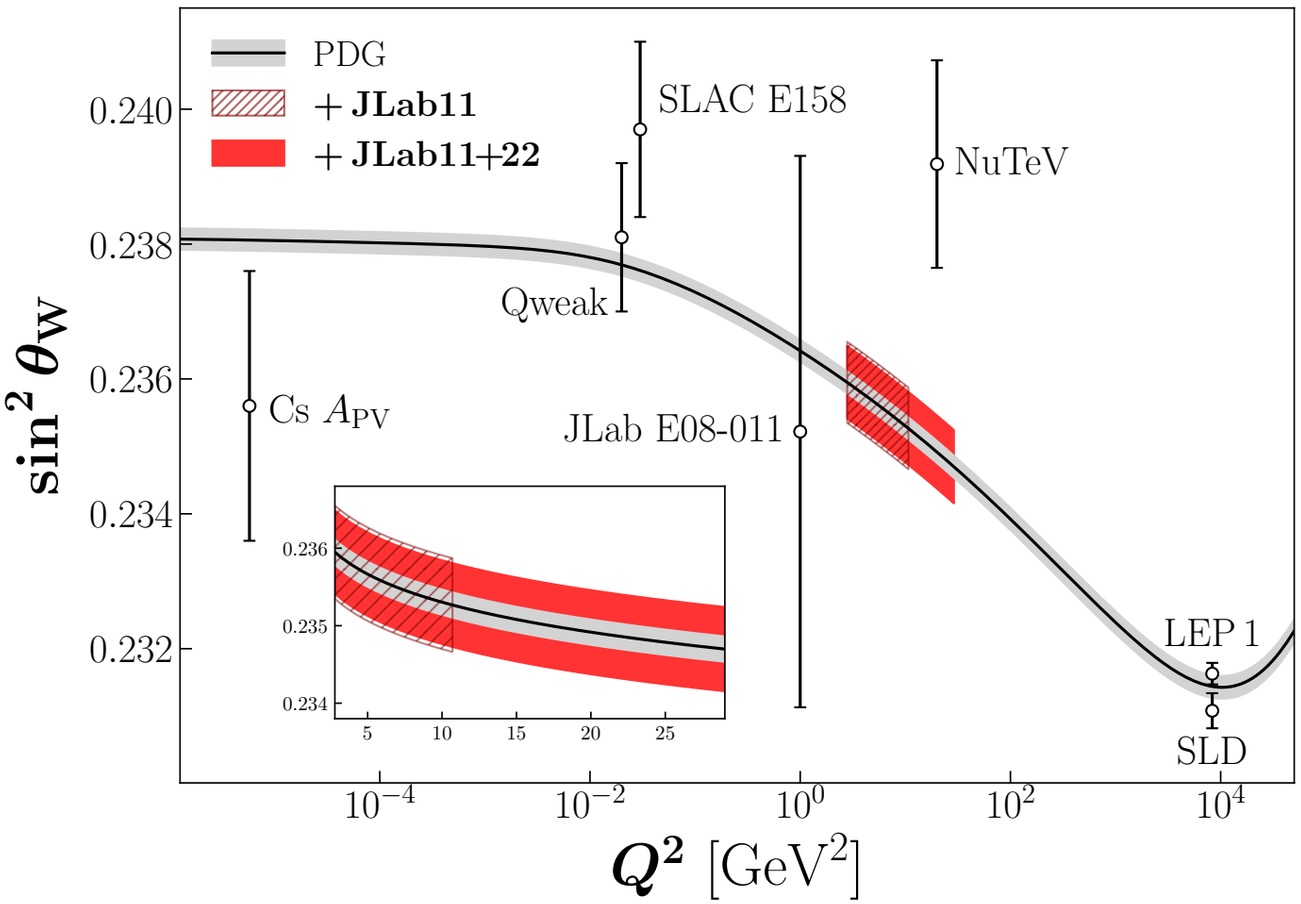
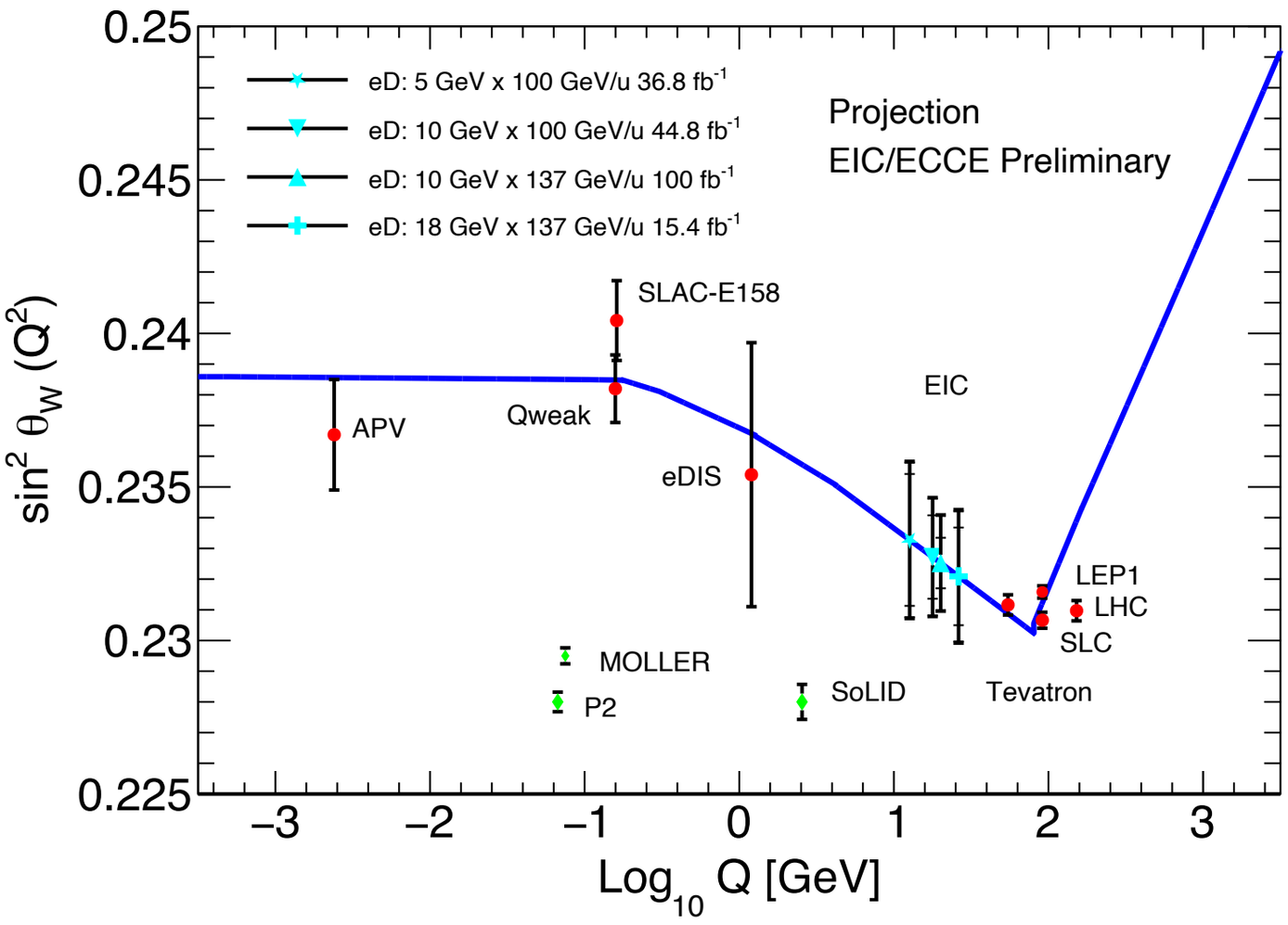


FIG. 11. Running of $\sin^2\theta_W$ (in the $\overline{\text{MS}}$ scheme) with energy scale Q^2 compared with selected experimental measurements. The value at the Z pole is provided by Ref. [14] through an average of the LEP 1 and SLD measurements. The red bands show uncertainties for $\sin^2\theta_W$ from simultaneous fits of $\sin^2\theta_W$ and unpolarized PDFs to simulated SoLID pseudodata across the range of Q^2 permitted by the pseudodata.

Extraction of the Weak Mixing Angle



[Boughezal, Emmert, Kutz, SM, Nycz, Petriello, Simsek, Wiegand, Zheng]

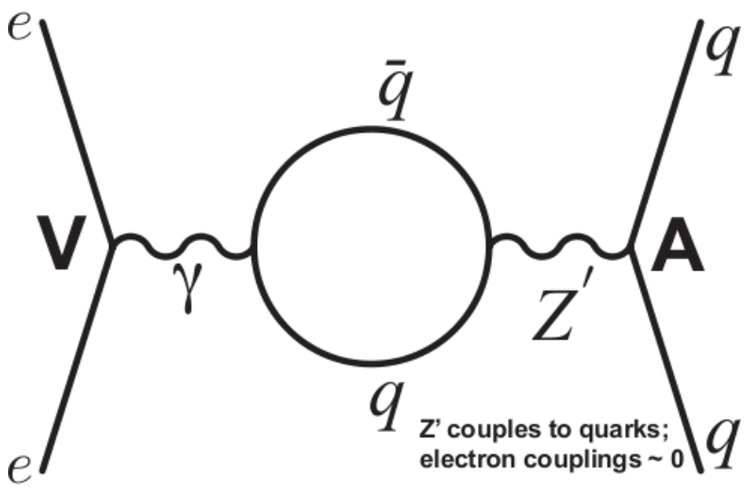
- SoLID can extract the weak mixing angle with higher precision than the EIC.

BSM Scenarios

Leptophobic Z'

- Leptophobic Z's are an interesting BSM scenario since they only shift the C_{2q} couplings in A_{PV}

- Leptophobic Z's only affect the $a_3(x)$ term or the C_{2q} coefficients in A_{PV}:

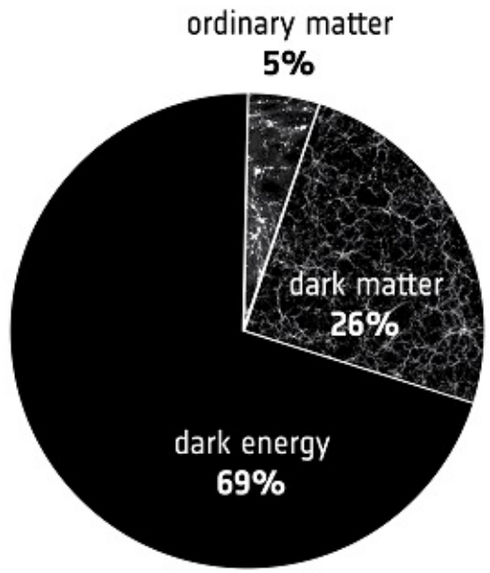


Leptophobic Z' contributes only to the C_{2q} couplings!

[M.Alonso-Gonzalez, M.Ramsey-Musolf; M.Buckley,M.Ramsey-Musolf]

$$A_{\mathrm{PV}}^{\mathrm{DIS}} = \frac{G_F Q^2}{4\sqrt{2}(1+Q^2/M_Z^2)\pi\alpha}\left[a_1 + \frac{1-(1-y)^2}{1+(1-y)^2}a_3\right]$$

Probing the Dark Sector



- Strong evidence for dark matter through gravitational effects:
  - Galactic Rotation Curves
  - Gravitational Lensing
  - Cosmic Microwave Background
  - Large Scale Structure Surveys

- WIMP dark matter paradigm
  - Mass ~ TeV
  - Weak interaction strength couplings
  - Gives the required relic abundance

- However, so far no direct evidence for WIMP dark matter

- Perhaps dark sector has a rich structure including different species and gauge forces, just like the visible sector

Dark Photon

- Dark $U(1)_d$ gauge group

- Interacts with SM via kinetic mixing (and mass mixing)

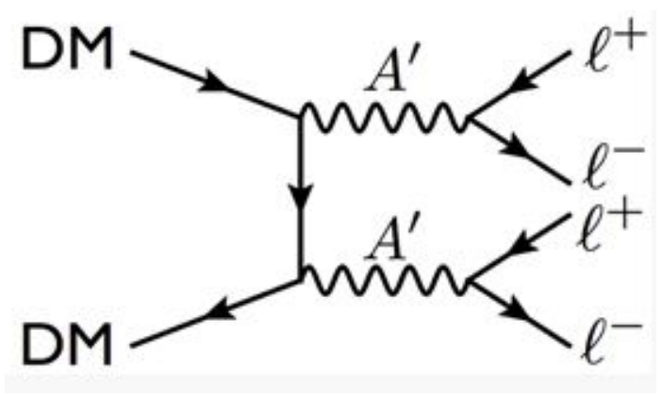
$$\mathcal{L} \supset -\frac{1}{4} F'_{\mu\nu} F'^{\mu\nu} + \frac{m^2_{A'}}{2} A'_\mu A'^\mu + \frac{\epsilon}{2\cos\theta_W} F'_{\mu\nu} B^{\mu\nu}$$

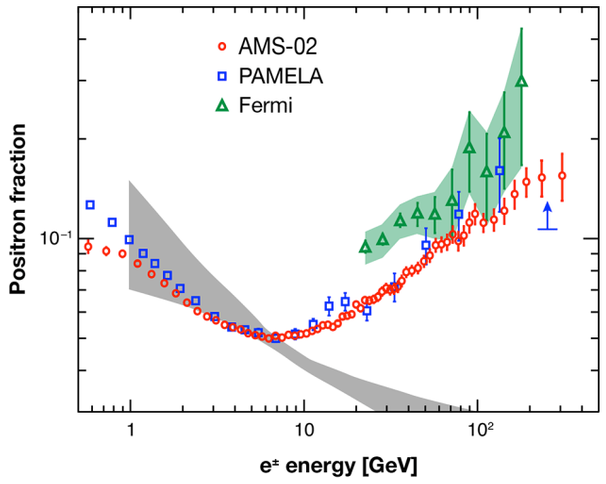
- The mixing induces a coupling of the dark photon to the electromagnetic and weak neutral currents.

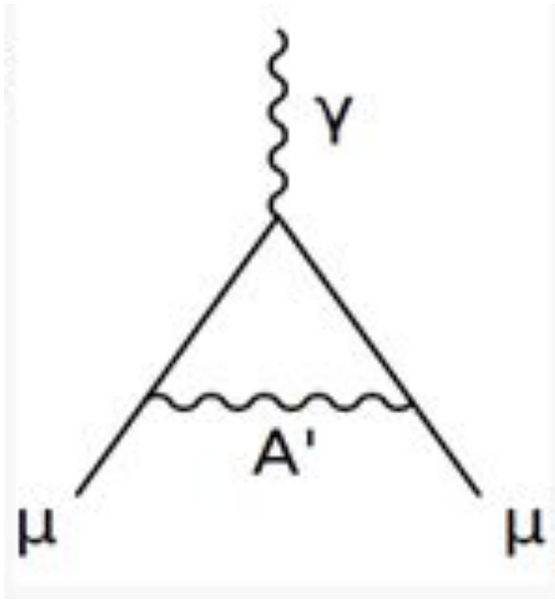
$$\mathscr{L}_{int} = -e\epsilon J^\mu_{em} A'_\mu$$

- Could help explain astrophysical data and anomalies

[Arkani-Hamed, Finkbeiner, Slatyer, Wiener, …]



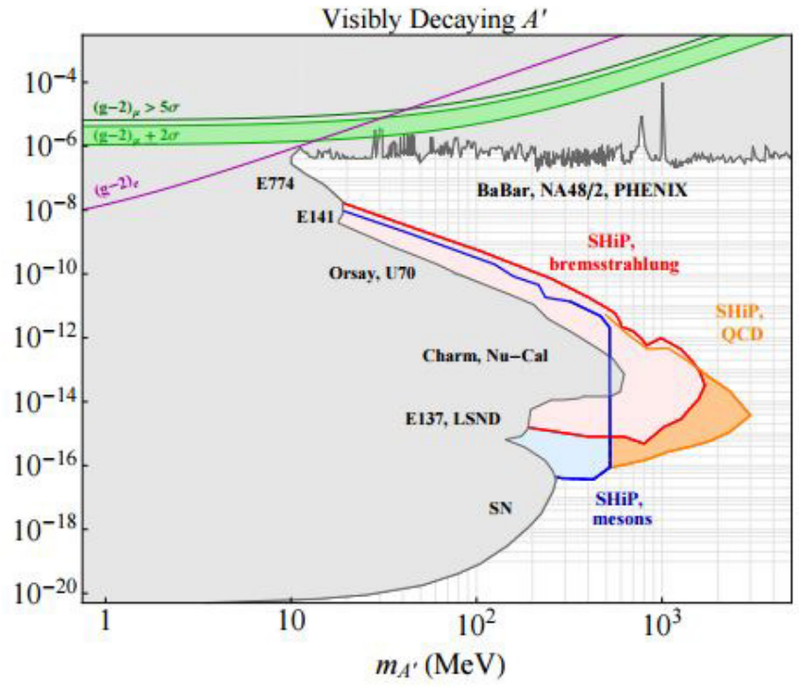




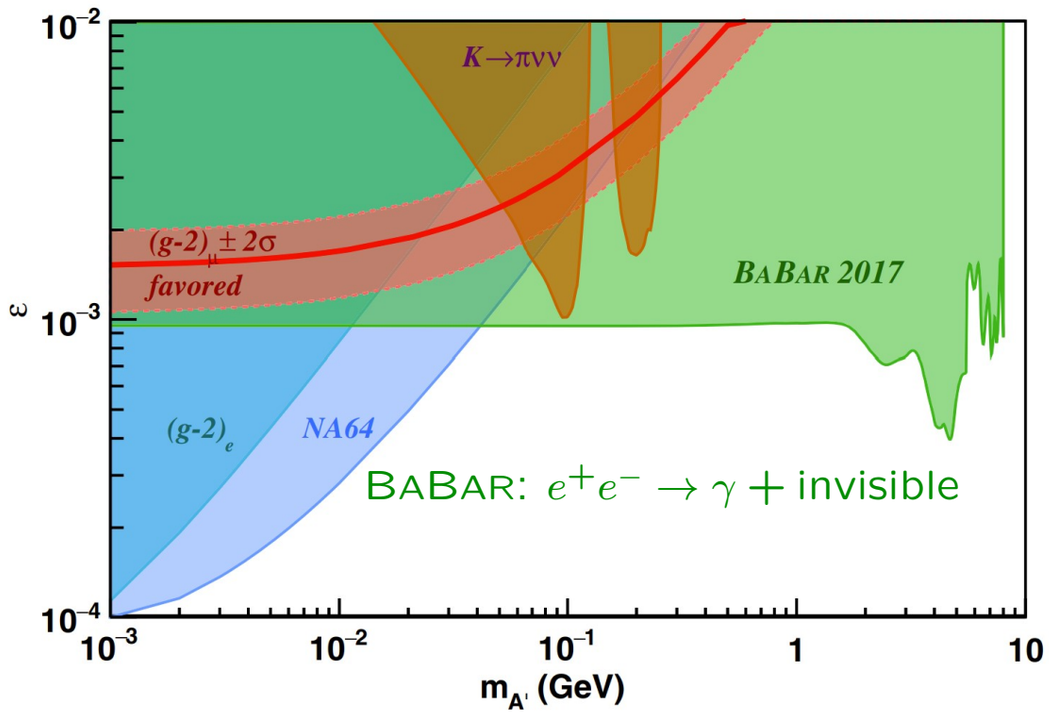
Dark Photon Scenario

- Active experimental program to search for dark photons

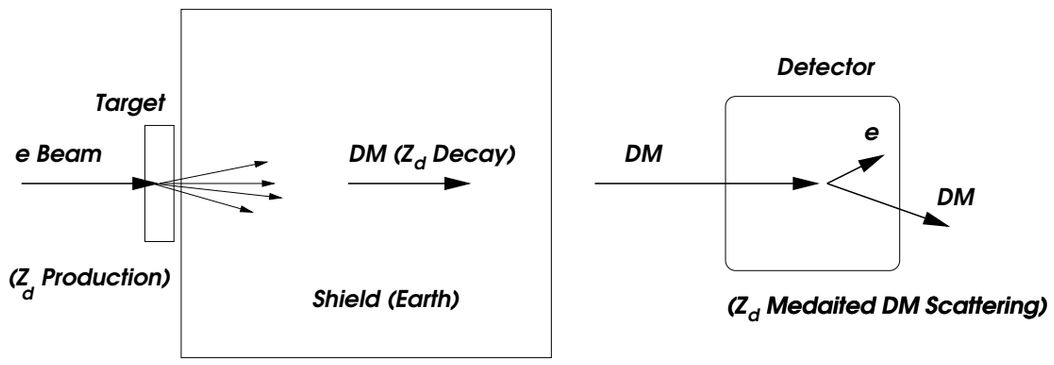
[Bjorken, Essig, Schuster, Toro; Baten, Pospelov, Ritz; Izaguirre Krnjaic, Schuster, Toro]



S. Alekhin *et al.*, arXiv:1504.04855 [hep-ph]



- Beam Dump Experiments:



[Bjorken, Essig, Schuster, Toro]

Impact of PVES on Dark Photon

[Thomas, Wang, Williams]

$$\mathcal{L} \supset -\frac{1}{4} F'_{\mu\nu} F'^{\mu\nu} + \frac{m^2_{A'}}{2} A'_\mu A'^\mu + \frac{\epsilon}{2\cos\theta_W} F'_{\mu\nu} B^{\mu\nu}$$

- Constraints on Dark Photon parameter space will be independent of the details of the decay branching fractions of the dark photon

- For a light dark photon, the induced coupling to the weak neutral coupling is suppressed (due to a cancellation between the kinetic and mass mixing induced couplings). [Gopalakrishna, Jung, Wells; Davoudiasl, Lee, Marciano]

- Thus, we consider a heavier dark photon for a sizable coupling to the weak neutral current and a correspondingly sizable effect in PVES. [Thomas, Wang, Williams]

Dark Photon Scenario: Shift in C_{1q} (PREX)

[Thomas, Wang, Williams]

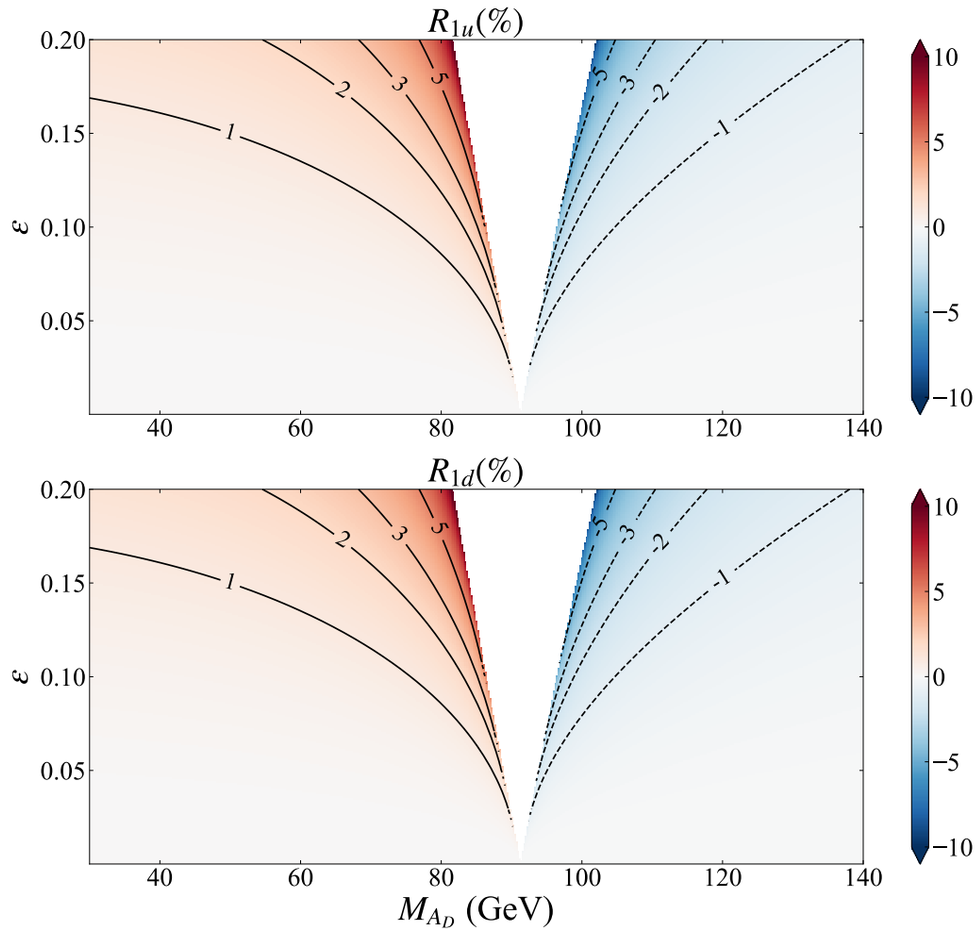


FIG. 1. The correction factors R_{1u} and R_{1d} at $Q^2 = 0.00616\ \mathrm{GeV}^2$, appropriate to the PREX-II experiment. The gap on the $\epsilon - M$ plane is not accessible because of "eigenmass repulsion" associated with the Z mass.

$$Q_W^p = -2\left[C_{1u}(2Z+N) + C_{1d}(Z+2N)\right]$$

$$C_{1q} = C_{1q}^{SM}(1+R_q)$$

- $R_{1q} \sim 4\,\%$ can lead to smaller extracted value for neutron radius, enough to eliminate tensions between the PREX measurements and theoretical model predictions.

Impact of PVES on Dark Photon

[Thomas, Wang, Williams]

$$\mathcal{L} \supset -\frac{1}{4}F'_{\mu\nu}F'^{\mu\nu} + \frac{m^2_{A'}}{2}A'_\mu A'^\mu + \frac{\epsilon}{2\cos\theta_W}F'_{\mu\nu}B^{\mu\nu}$$

- Constraints on Dark Photon parameter space will be independent of the details of the decay branching fractions of the dark photon

- The usual PVDIS asymmetry has the form:

$$A_{\rm PV}^{\rm DIS} = \frac{G_F Q^2}{4\sqrt{2}(1+Q^2/M_Z^2)\pi\alpha}\left[a_1 + \frac{1-(1-y)^2}{1+(1-y)^2}a_3\right]$$

- Including the effects of a dark photon, we get additional terms:

$$A_{\rm PV} = \frac{Q^2}{2\sin^2 2\theta_W(Q^2+M_Z^2)}\left[a_1^{\gamma Z} + \frac{1-(1-y)^2}{1+(1-y)^2}a_3^{\gamma Z}\right.$$
$$\left. + \frac{Q^2+M_Z^2}{Q^2+M_{A_D}^2}\left(a_1^{\gamma A_D} + \frac{1-(1-y)^2}{1+(1-y)^2}a_3^{\gamma A_D}\right)\right],$$

Dark Photon Scenario: Shift in C_{iq} (PVDIS, HERA)

[Thomas, Wang, Williams]

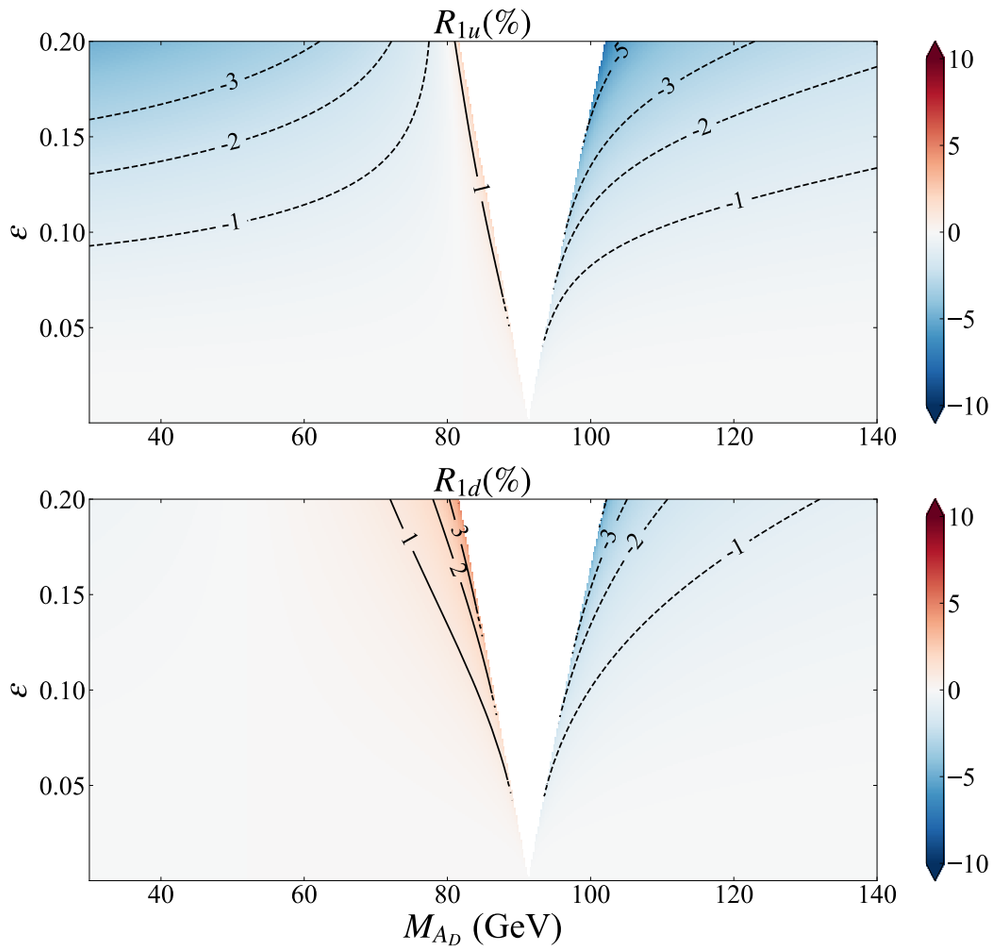


FIG. 2. The correction factors R_{1u} and R_{1d} at $Q^2 = M_Z^2$.

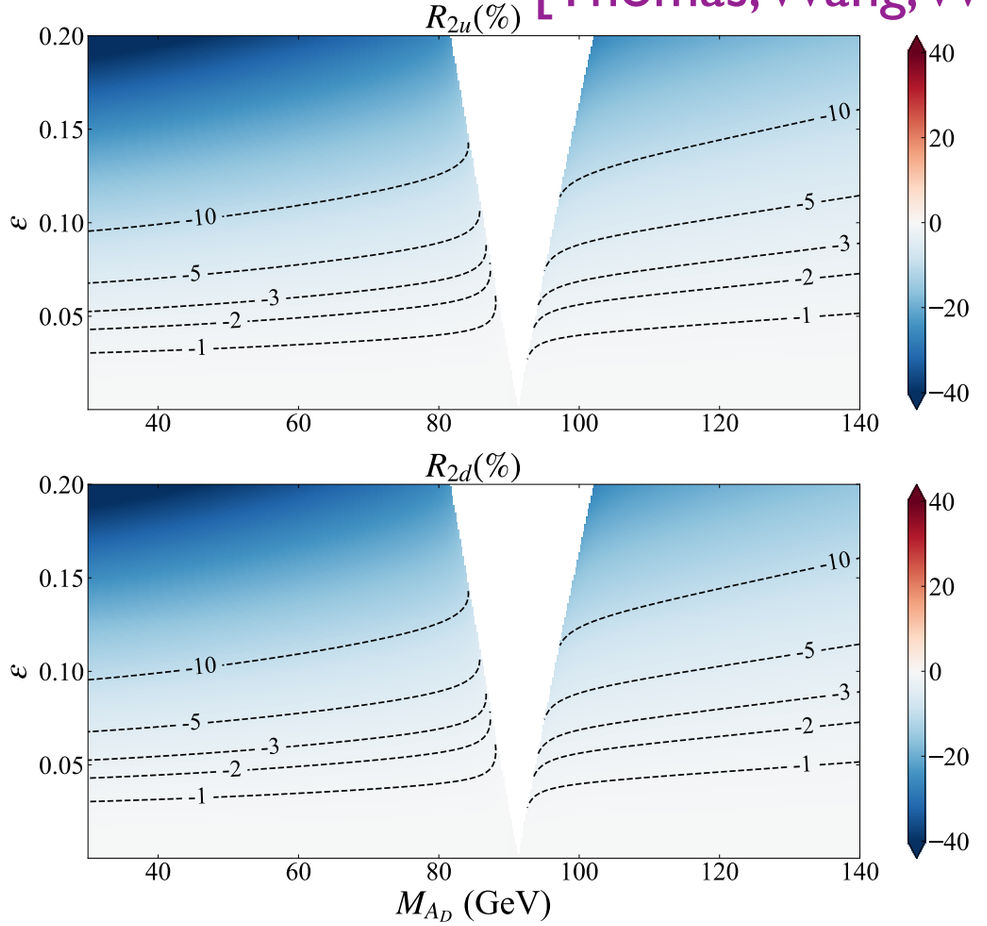


FIG. 3. The correction factors R_{2u} and R_{2d} at $Q^2 = M_Z^2$.

$$C_{1q} = C_{1q}^Z + \frac{Q^2 + M_Z^2}{Q^2 + M_{A_D}^2} C_{1q}^{A_D} = C_{1q}^{\rm SM}(1 + R_{1q})$$

$$C_{2q} = C_{2q}^Z + \frac{Q^2 + M_Z^2}{Q^2 + M_{A_D}^2} C_{2q}^{A_D} = C_{2q}^{\rm SM}(1 + R_{2q})$$

- PVDIS measurements provide independent probes of dark photons, complementary to PREX and searches for invisible and visible dark photons.

Dark Photon Scenario: Shift in C_{iq} (PVDIS)

Qualitatively different behavior in shifts to C_{iq} for different Q^2

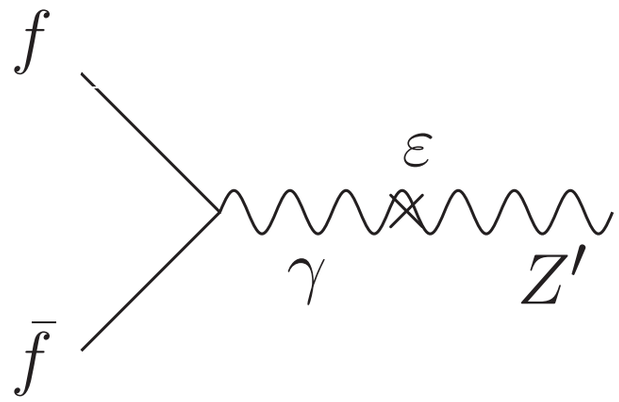
Useful to explore dark-photon space over a wide range of Q^2

Estimates for the sensitivity of PVDIS at SoLID kinematics and luminosity should be made. Easy to do with the already established formalism.

Light Dark-Z Parity Violation

[Davoudiasl, Lee, Marciano]

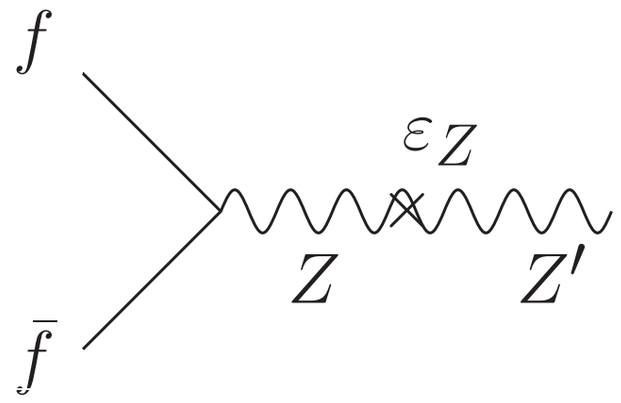
- An interesting scenario is that of a "light" Dark-Z.



- The standard kinetic mixing scenario:

$$\mathcal{L}_{\text{gauge}} = -\frac{1}{4}B_{\mu\nu}B^{\mu\nu} + \frac{1}{2}\frac{\varepsilon}{\cos\theta_W}B_{\mu\nu}Z_d^{\mu\nu} - \frac{1}{4}Z_{d\mu\nu}Z_d^{\mu\nu}$$

- And additional mass mixing (for example, from extended Higgs sector) to induce sizable dark-Z coupling to the weak neutral current:



$$M_0^2 = m_Z^2 \begin{pmatrix} 1 & -\varepsilon_Z \\ -\varepsilon_Z & m_{Z_d}^2/m_Z^2 \end{pmatrix}$$

$$\varepsilon_Z = \frac{m_{Z_d}}{m_Z}\delta$$

- Dark-Z couples to the electromagnetic and neutral current coupling:

$$\mathcal{L}_{\text{int}} = \left(-e\varepsilon J_\mu^{em} - \frac{g}{2\cos\theta_W}\varepsilon_Z J_\mu^{NC}\right) Z_d^\mu$$

Light Dark-Z Parity Violation

[Davoudiasl, Lee, Marciano]

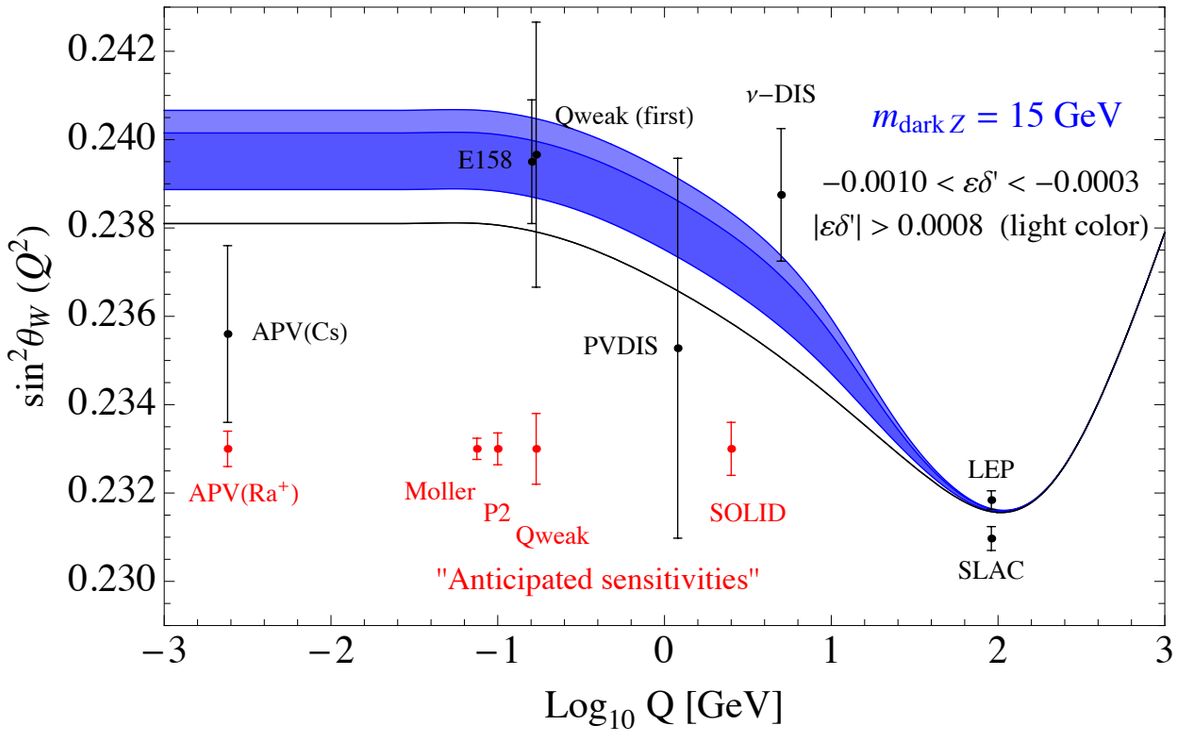
- Effective change in presence of dark-Z for parity violating asymmetries:

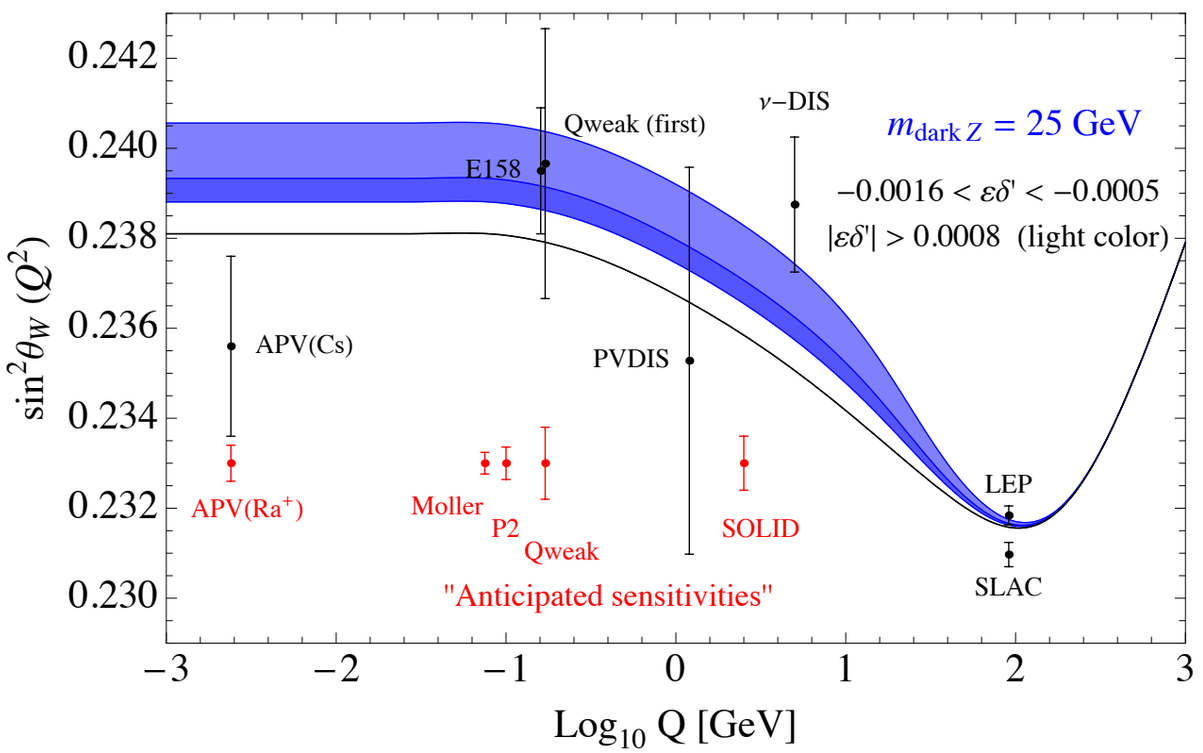
$$G_F \to \rho_d G_F$$

$$\sin^2\theta_W \to \kappa_d \sin^2\theta_W$$

$$\rho_d = 1 + \delta^2 \frac{m_{Z_d}^2}{Q^2 + m_{Z_d}^2}$$

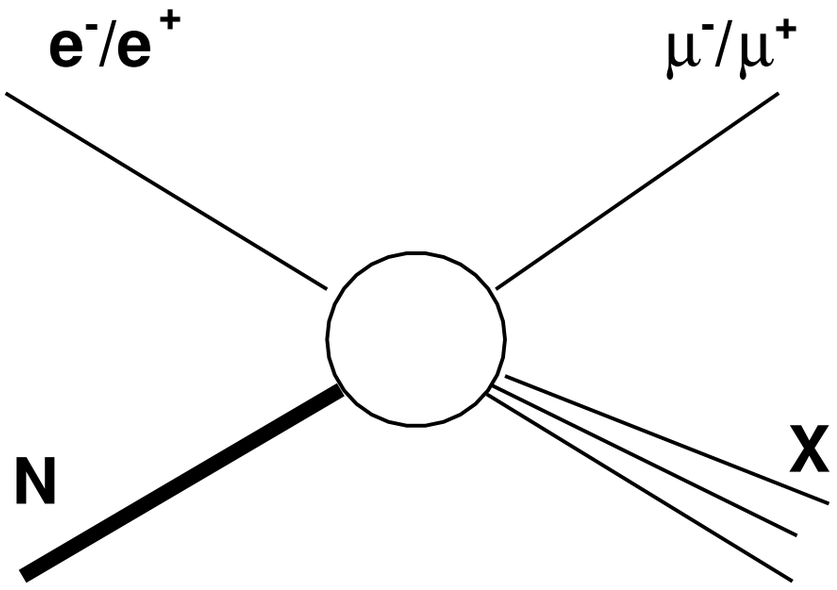
$$\kappa_d = 1 - \frac{\varepsilon}{\varepsilon_Z}\delta^2 \frac{\cos\theta_W}{\sin\theta_W} \frac{m_{Z_d}^2}{Q^2 + m_{Z_d}^2}$$





CLFV(1,2) in DIS

[Furletova, SM]



$$e^{\pm} + N \rightarrow \mu^{\pm} + X$$

- One can also search for CLFV(1,2) in the DIS process, which can probe different CLFV mechanisms and is complementary to the other low energy experiments.

- There are already CLFV(1,2) limits from the $H1$ and ZEUS collaborations at HERA. For example, the $H1$ collaboration made searches for the settings:

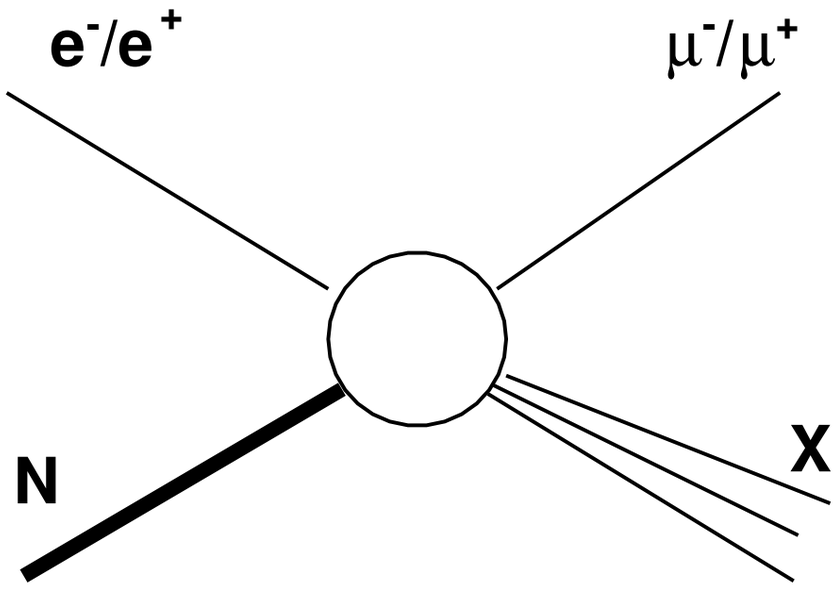
[S. Chekanov et.al (ZEUS), A.Atkas et.al (H1)]

$$\sqrt{s} = 319\ \text{GeV}$$

$$H1, e^{-}p : \mathscr{L} = 166\ \text{pb}^{-1}$$

$$H1, e^{+}p : \mathscr{L} = 245\ \text{pb}^{-1}$$

CLFV(1,2) in DIS



$$e^{\pm} + N \rightarrow \mu^{\pm} + X$$

- One can also set limits on CLFV(1,2) at JLAB:

$$\sqrt{s} = 4.5\ \text{GeV} \qquad \text{JLAB} : \mathscr{L} = 10^{36-39}\ \text{cm}^{-2}\ s^{-1}$$

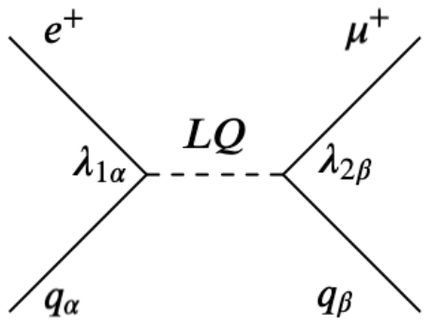
- Even though the center of mass energy is very small compared to HERA, corresponding to a much lower mass reach, the much larger luminosity could allow for improvement over HERA by up to two orders of magnitude.

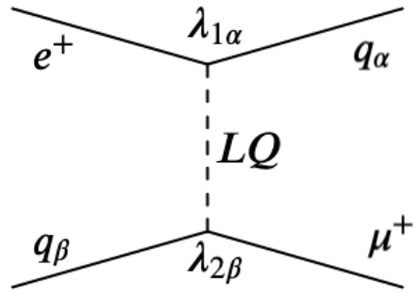
Preliminary Estimates of CLFV Limits at JLAB

Type	J	F	Q	ep dominant process	Coupling	Branching ratio β_ℓ
S_0^L	0	2	$-1/3$	$e_L^- u_L \to \begin{cases} \ell^- u \\ \nu_\ell d \end{cases}$	λ_L $-\lambda_L$	1/2 1/2
S_0^R	0	2	$-1/3$	$e_R^- u_R \to \ell^- u$	λ_R	1
$\tilde{S}_0^R$	0	2	$-4/3$	$e_R^- d_R \to \ell^- d$	λ_R	1
S_1^L	0	2	$-1/3$ $-4/3$	$e_L^- u_L \to \begin{cases} \ell^- u \\ \nu_\ell d \end{cases}$ $e_L^- d_L \to \ell^- d$	$-\lambda_L$ $-\lambda_L$ $-\sqrt{2}\lambda_L$	1/2 1/2 1
$V_{1/2}^L$	1	2	$-4/3$	$e_L^- d_R \to \ell^- d$	λ_L	1
$V_{1/2}^R$	1	2	$-1/3$ $-4/3$	$e_R^- u_L \to \ell^- u$ $e_R^- d_L \to \ell^- d$	λ_R λ_R	1 1
$\tilde{V}_{1/2}^L$	1	2	$-1/3$	$e_L^- u_R \to \ell^- u$	λ_L	1

Type	J	F	Q	ep dominant process	Coupling	Branching ratio β_ℓ
V_0^L	1	0	$+2/3$	$e_R^+ d_L \to \begin{cases} \ell^+ d \\ \bar{\nu}_\ell u \end{cases}$	λ_L λ_L	1/2 1/2
V_0^R	1	0	$+2/3$	$e_L^+ d_R \to \ell^+ d$	λ_R	1
$\tilde{V}_0^R$	1	0	$+5/3$	$e_L^+ u_R \to \ell^+ u$	λ_R	1
V_1^L	1	0	$+2/3$ $+5/3$	$e_R^+ d_L \to \begin{cases} \ell^+ d \\ \bar{\nu}_\ell u \end{cases}$ $e_R^+ u_L \to \ell^+ u$	$-\lambda_L$ λ_L $\sqrt{2}\lambda_L$	1/2 1/2 1
$S_{1/2}^L$	0	0	$+5/3$	$e_R^+ u_R \to \ell^+ u$	λ_L	1
$S_{1/2}^R$	0	0	$+2/3$ $+5/3$	$e_L^+ d_L \to \ell^+ d$ $e_L^+ u_L \to \ell^+ u$	$-\lambda_R$ λ_R	1 1
$\tilde{S}_{1/2}^L$	0	0	$+2/3$	$e_R^+ d_R \to \ell^+ d$	λ_L	1

[Furletova, SM]





- Limits based on running for 5 years with instantaneous luminosity of $\mathscr{L} \sim 10^{38}\,\mathrm{cm}^{-2}s^{-1}$. For an integrated luminosity a factor of 10 smaller, there is still substantial room for improvement over HERA limits.

- Thus, JLAB could improve on HERA limits by two or three orders of magnitude: $z \sim [0.005 - 0.05]$

- This estimate will be modified after taking into account acceptance and background effects.

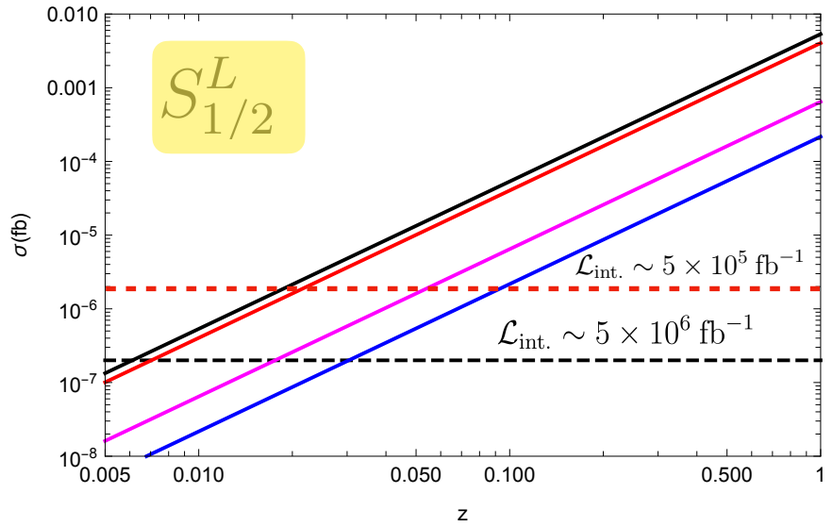


Fig. 5. The cross section for $e^+N \to \mu^+X$ with center of mass energy $\sqrt{s} = 4.5$ GeV, via exchange of the F=0 scalar LQ, $S_{1/2}^L$, as a function of the ratio z defined in Eq. (9). The red, black, magenta, and blue solid lines correspond to the choices $(\alpha, \beta) = \{11, 12, 21, 22\}$ in Eq. (6) with all other terms set to zero. An integrated luminosity of $\mathcal{L} \sim 5 \times 10^6 \mathrm{fb}^{-1}$ will allow sensitivity to cross sections as small as $\sigma \sim 0.2 \times 10^{-6}$ fb (horizontal dashed line).

SMEFT Analysis

Standard Model Effective Theory (SMEFT) Operator Basis [Boughezal, Petriello, Wiegand]

- The SMEFT framework can be used to constrain new physics beyond the electroweak scale in a model-independent manner:

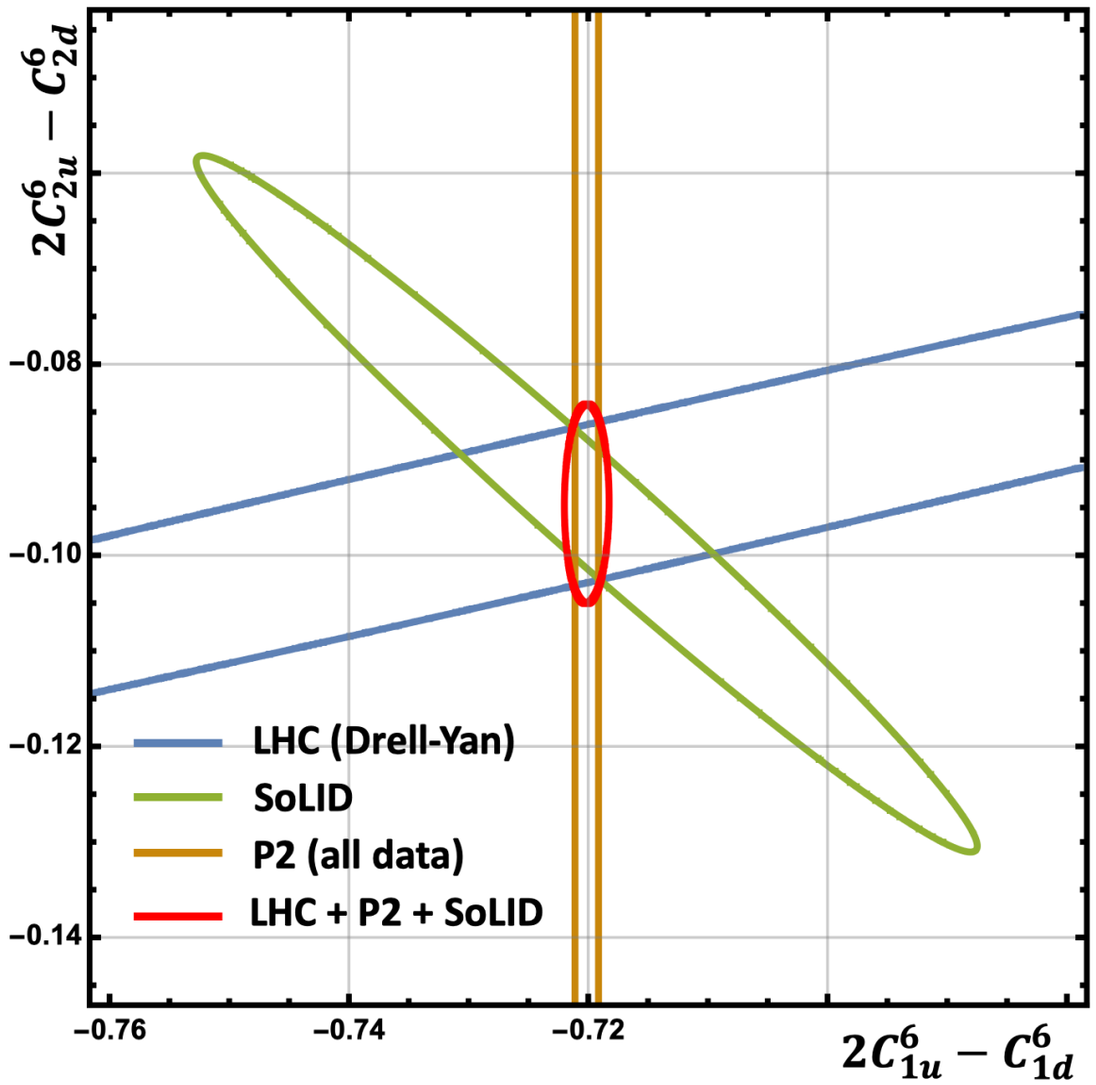
$$\mathcal{L} = \mathcal{L}_{SM} + \frac{1}{\Lambda^2}\sum_i C_i^6 \mathcal{O}_{6,i} + \frac{1}{\Lambda^4}\sum_i C_i^8 \mathcal{O}_{8,i} + \dots$$

- Relevant SMEFT operators for DIS processes at dim-6 and dim-8

Dimension 6		Dimension 8	
$\mathcal{O}_{lq}^{(1)}$	$\left(\bar{l}\gamma^\mu l\right)\left(\bar{q}\gamma_\mu q\right)$	$\mathcal{O}_{l^2q^2D^2}^{(1)}$	$D^\nu\left(\bar{l}\gamma^\mu l\right) D_\nu\left(\bar{q}\gamma_\mu q\right)$
$\mathcal{O}_{lq}^{(3)}$	$\left(\bar{l}\gamma^\mu \tau^i l\right)\left(\bar{q}\gamma_\mu \tau^i q\right)$	$\mathcal{O}_{l^2q^2D^2}^{(3)}$	$D^\nu\left(\bar{l}\gamma^\mu \tau^i l\right) D_\nu\left(\bar{q}\gamma_\mu \tau^i q\right)$
$\mathcal{O}_{eu}$	$\left(\bar{e}\gamma^\mu e\right)\left(\bar{u}\gamma_\mu u\right)$	$\mathcal{O}_{e^2u^2D^2}^{(1)}$	$D^\nu\left(\bar{e}\gamma^\mu e\right) D_\nu\left(\bar{u}\gamma_\mu u\right)$
$\mathcal{O}_{ed}$	$\left(\bar{e}\gamma^\mu e\right)\left(\bar{d}\gamma_\mu d\right)$	$\mathcal{O}_{e^2d^2D^2}^{(1)}$	$D^\nu\left(\bar{e}\gamma^\mu e\right) D_\nu\left(\bar{d}\gamma_\mu d\right)$
$\mathcal{O}_{lu}$	$\left(\bar{l}\gamma^\mu l\right)\left(\bar{u}\gamma_\mu u\right)$	$\mathcal{O}_{l^2u^2D^2}^{(1)}$	$D^\nu\left(\bar{l}\gamma^\mu l\right) D_\nu\left(\bar{u}\gamma_\mu u\right)$
$\mathcal{O}_{ld}$	$\left(\bar{l}\gamma^\mu l\right)\left(\bar{d}\gamma_\mu d\right)$	$\mathcal{O}_{l^2d^2D^2}^{(1)}$	$D^\nu\left(\bar{l}\gamma^\mu l\right) D_\nu\left(\bar{d}\gamma_\mu d\right)$
$\mathcal{O}_{qe}$	$\left(\bar{q}\gamma^\mu q\right)\left(\bar{e}\gamma_\mu e\right)$	$\mathcal{O}_{q^2e^2D^2}^{(1)}$	$D^\nu\left(\bar{q}\gamma^\mu q\right) D_\nu\left(\bar{e}\gamma_\mu e\right)$

Lifting Flat Directions

[Boughezal, Petriello, Wiegand]

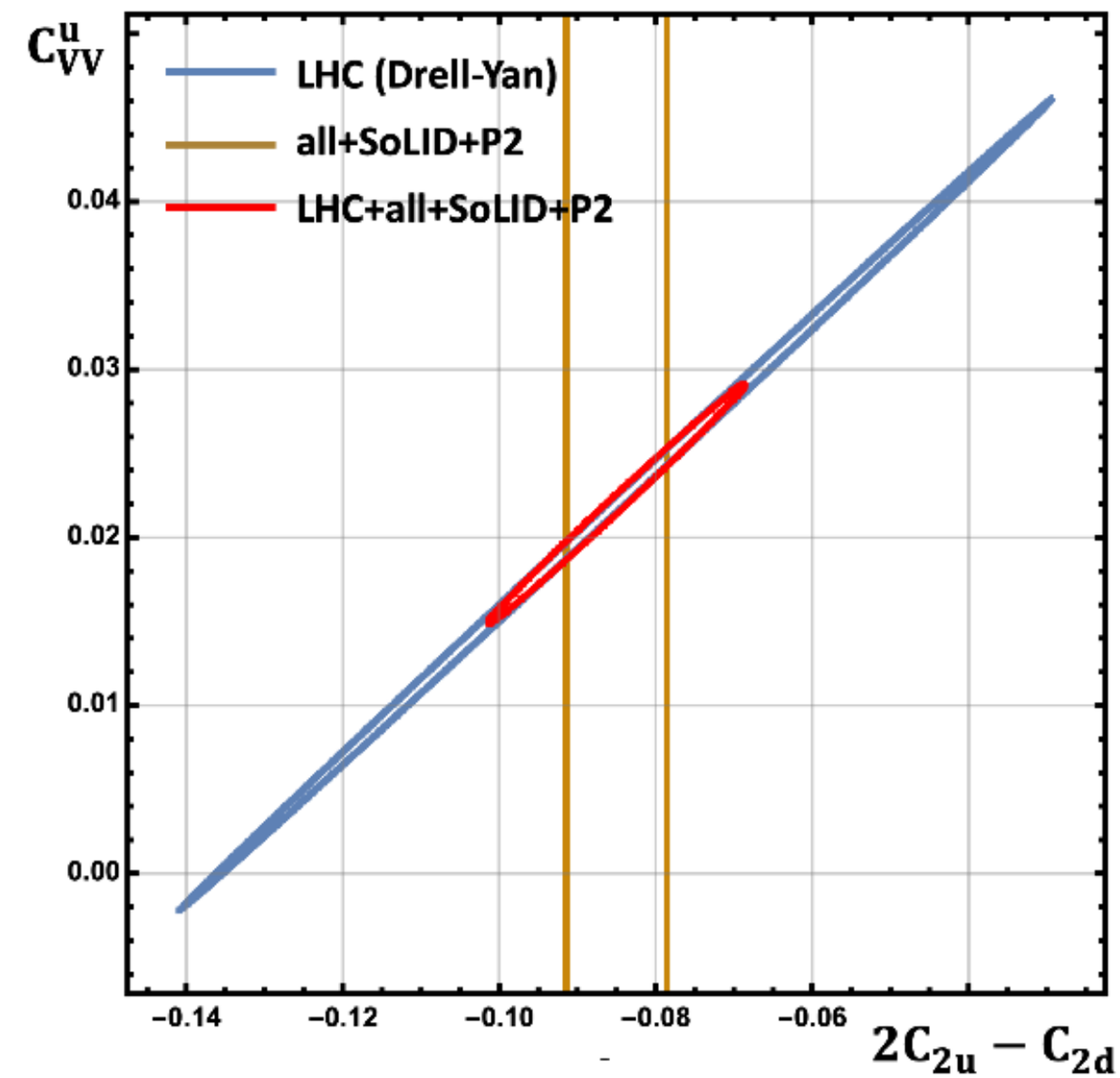


- PVES and Drell-Yan at the LHC are sensitive to different combinations of the SMEFT Wilson coefficients.

- PVES can lift "flat directions" by probing orthogonal directions in the SMEFT parameter space compared to the LHC

Lifting Flat Directions

[Boughezal, Petriello, Wiegand]

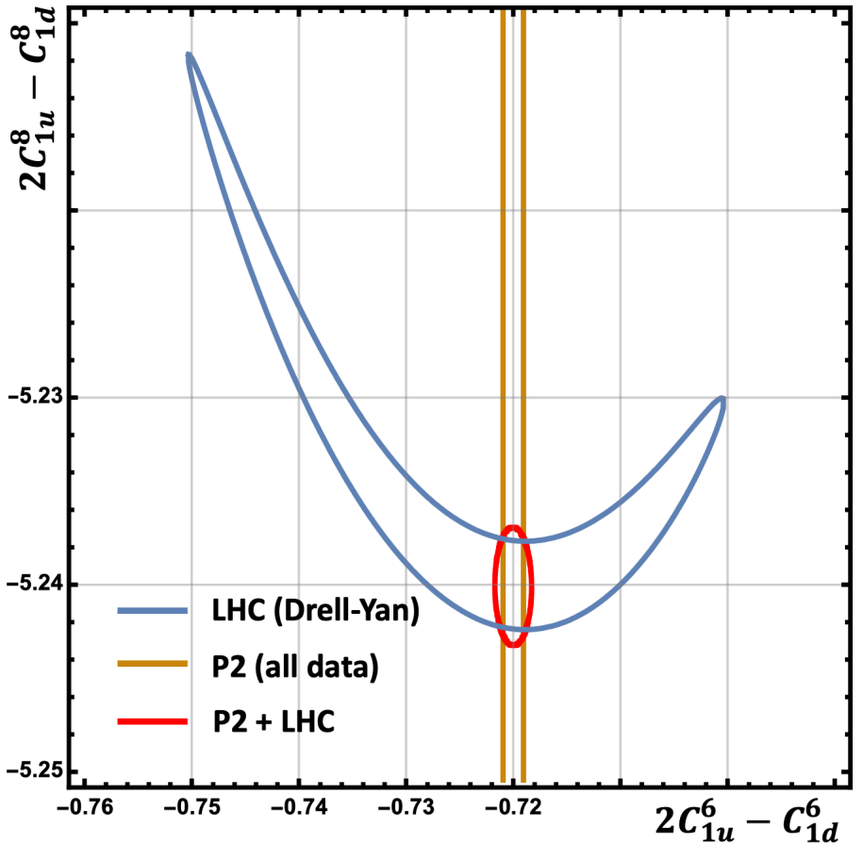


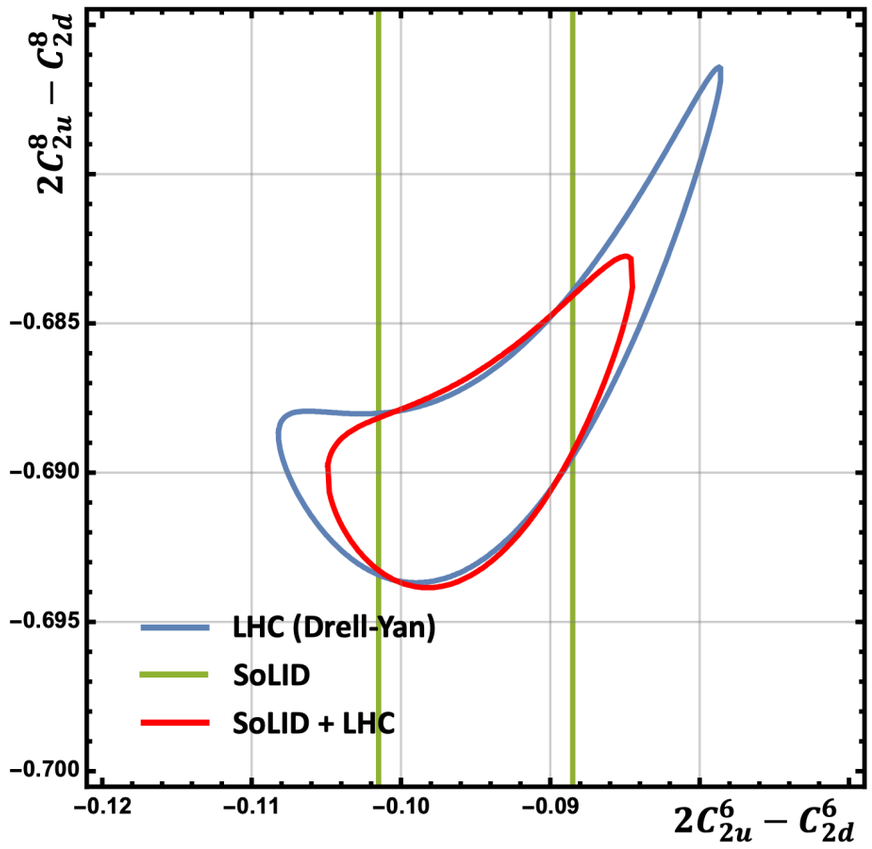
- An example of SOLID probing a unique direction in parameter space. Neither the LHC, Qweak, P2, or APV have sensitivity in this region

- This requires that $2C_{1u} - C_{1d}$ is assumed to be know from the P2 experiment so that the SOLID then directly measures $2C_{2u} - C_{2d}$

Disentangling Dim-6 and Dim-8 SMEFT Operators

[Boughezal, Petriello, Wiegand]





- Another advantage of low energy PVES experiments:

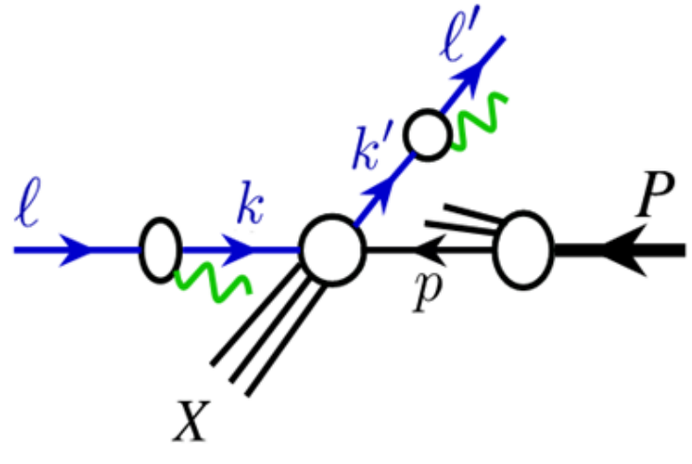
  The large energy of the LHC can make it difficult to disentangle the effects of dim-6 or dim-8 (and dim-6 squared) operators.

  Low energy PVES will only have sensitivity to dim-6 operators providing valuable input to disentangle dim-6 vs dim-8.

Collision-Induced QED Radiation Effects

• Collision induced QED radiation can result in a mismatch between the reconstructed and true values of the momentum transfer delivered.

• Can significantly affect theoretical predictions and the interpretation of data.



[Liu, Melnitchouk, Qiu, Sato; Cammarato, Qiu, Watanabe, Zhang]

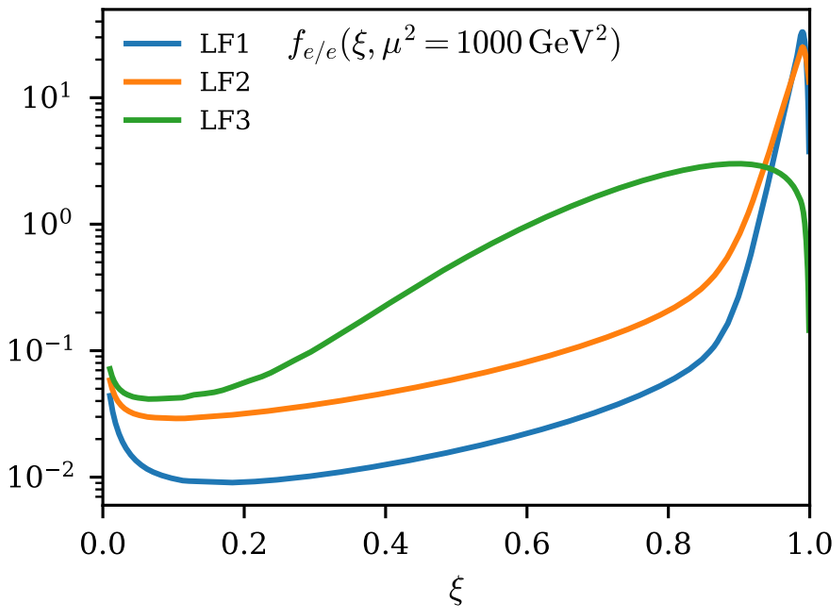
• Joint QCD+QED factorization approach treats QED radiation of electrons and quarks on an equal footing through the introduction of lepton distribution and fragmentation functions:

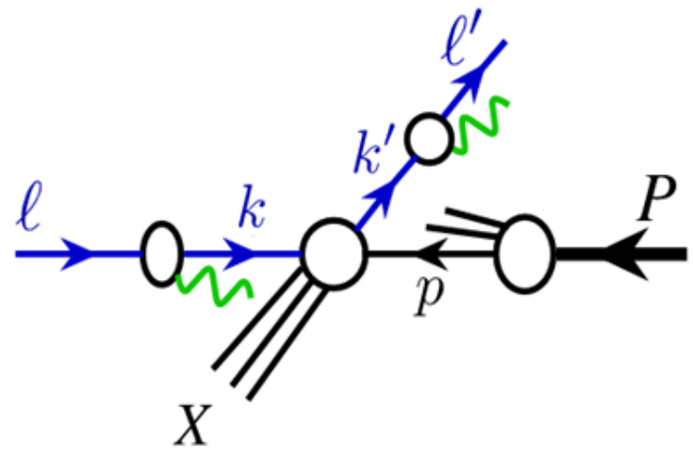
$$d\sigma \;=\; \frac{1}{2S}\sum_{i,j,a} D_{e/j}(\zeta,\mu)\otimes_\zeta \; f_{i/e}(\xi,\mu)\otimes_\xi \; f_{a/h}(x,\mu)\otimes_x \hat{H}_{ia\to jX}(\hat{s},\hat{t},\hat{u},\mu)$$

• QED radiation is treated as a contribution to the cross section rather than effect that must be subtracted.

Collision-Induced QED Radiation Effects on Cross Section and Asymmetries

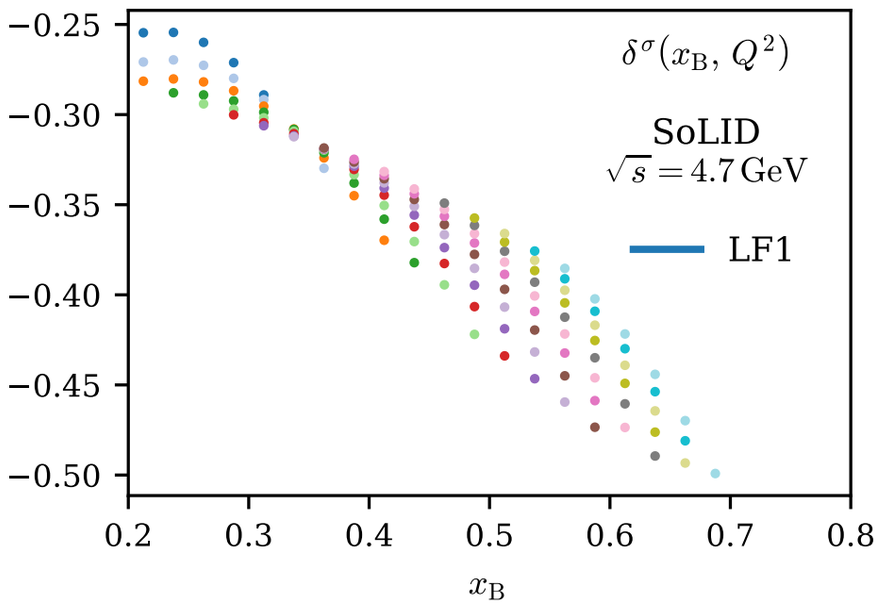
- Lepton distribution functions:





[Liu, Melnitchouk, Qiu, Sato; Cammarato, Qiu, Watanabe, Zhang]

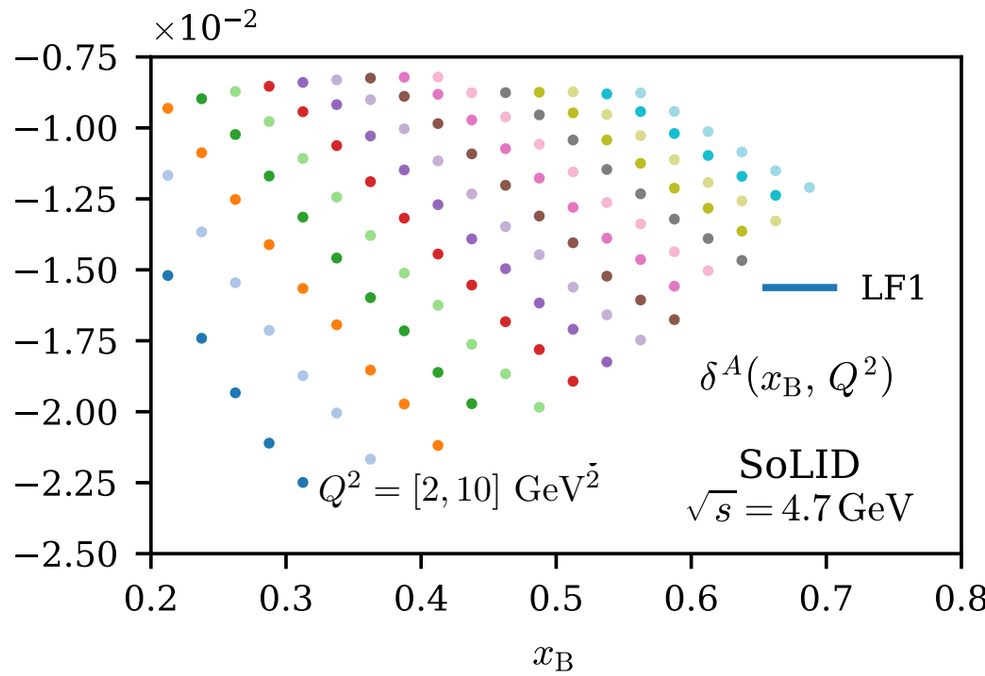
- Impact on cross sections and PVDIS asymmetry:



[SM, Qiu, Zhang]

$$d\sigma_0 = d\sigma_0^{\mathrm{NR}}\,(1+\delta^\sigma)$$
$$A_e = A_e^{\mathrm{NR}}\,(1+\delta^A)$$

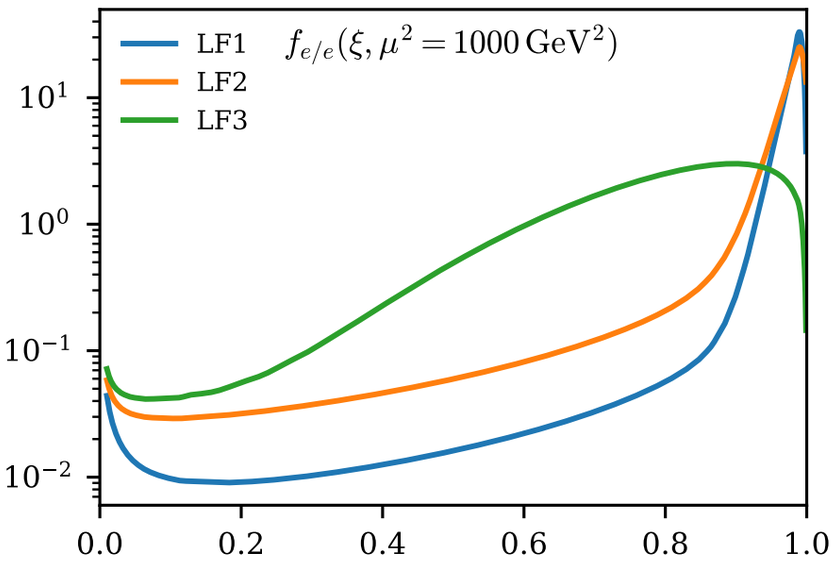
$Q^2 = [2, 10]\ \mathrm{GeV}^2$
$\Delta Q^2 = 0.5\,\mathrm{GeV}^2$

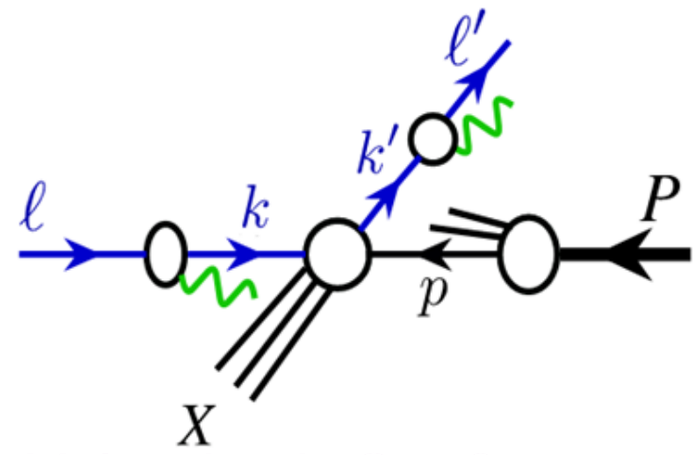


- Asymmetries are relatively more robust to the effects of QED radiation.

Collision-Induced QED Radiation Effects on SMEFT Constraints

- Lepton distribution functions:

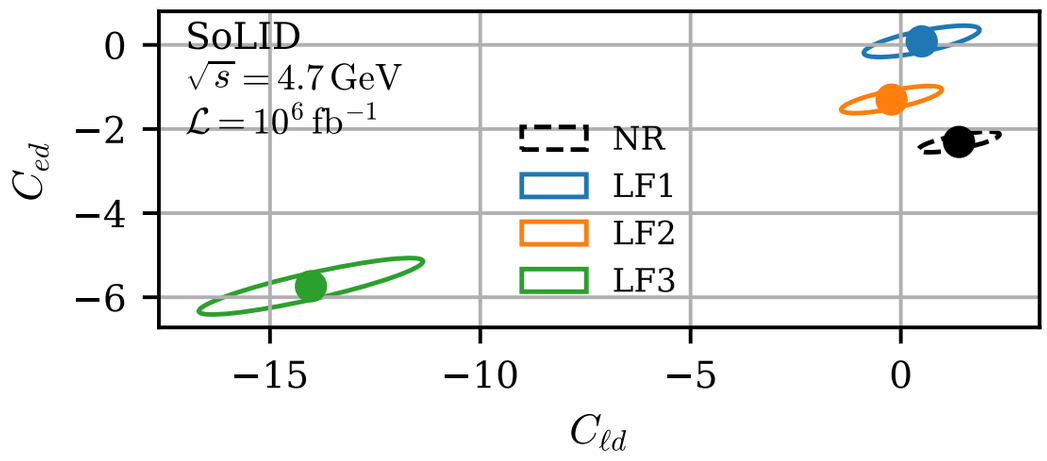




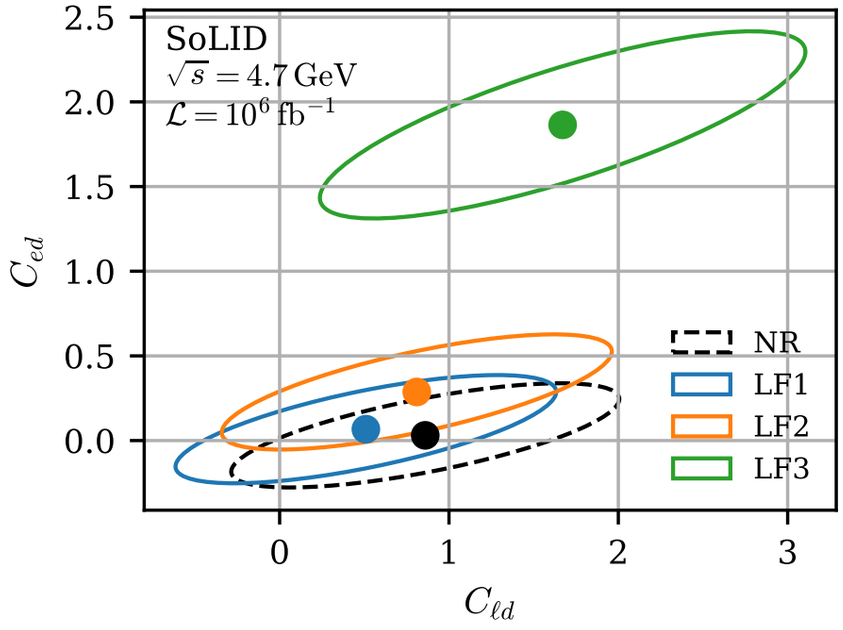
[Liu, Melnitchouk, Qiu, Sato; Cammarato, Qiu, Watanabe, Zhang]

- Impact on extracted SMEFT Wilson Coefficients:

[SM, Qiu, Zhang]



cross section



asymmetry

- Asymmetries are more robust against the effects of QED radiation

Conclusions

- PVDIS with SoLID at JLAB can provide unique and complementary information to constrain new physics

- Allows for precision extractions of the weak mixing angle

- It can provide input for the global SMEFT analysis by lifting flat directions and disentangling dim-6 and dim-8 operators

- Can constrain the parameter space of Dark photons/Z and Leptophobic Z-primes

- Hadronic and QED radiation effects must be under control for a reliable interpretation of BSM constraints.

Back-Up Slides

C_{iq}, C_{2e} via Parity-Violating Electron Scattering (PVES)

- Parity-Violating asymmetry using longitudinally polarized electron beams, can probe C_{iq} and C_{2e}:

$$A_{RL} = \frac{\sigma_R - \sigma_L}{\sigma_R + \sigma_L}$$

Elastic Electron-Proton Scattering Asymmetry

• Low Energy and forward ($E \to 0$, $Q^2 \to 0$), elastic electron-proton scattering asymmetry is sensitive to the proton weak charge:

$$A_{RL} = -\frac{G_F Q^2}{4\pi\alpha\sqrt{2}}\left[Q_W^p - F(E, Q^2)\right]$$

proton weak charge Proton structure

• At tree-level, the SM value of the proton weak charge is (receives radiative corrections + box diagram corrections):

$$Q_W^p = -2\left[2C_{1u} + C_{1d}\right] = 1 - 4\sin^2\theta_W$$

	$Q^2(\mathrm{GeV}^2/\mathrm{c}^2)$	E	δQ_W^p	$\delta \sin^2\theta_W$
Q_{weak}	0.025	1.155 GeV	~ 4 %	~ 0.3 %
P2 (MESA)	0.006	155 MeV	~ 2 %	~ 0.15 %

Moller Scattering Asymmetry

• Low Energy and forward ($E \to 0$, $Q^2 \to 0$), elastic electron-electron scattering asymmetry is sensitive to the proton weak charge:

$$A_{RL} = \frac{G_F Q^2}{\sqrt{2}\pi\alpha}\left[\frac{1-y}{1+y^4+(1-y)^4}\right] Q_W^e$$

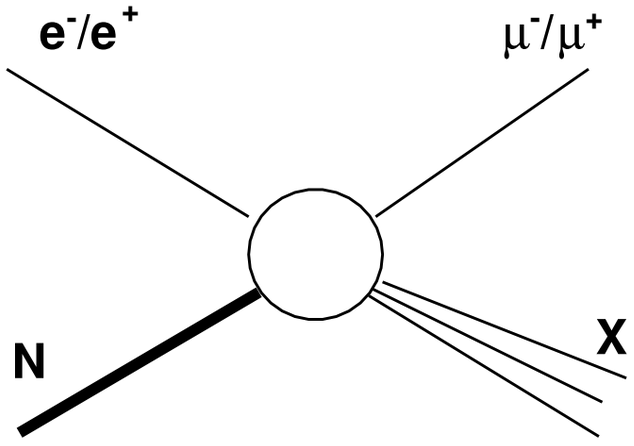
electron weak charge

• At tree-level, the SM value of the proton weak charge is (receives radiative corrections + box diagram corrections):

$$Q_W^e = -2C_{2e} = -1 + 4\sin^2\theta_W$$

	$Q^2(\mathrm{GeV}^2/c^2)$	E	δQ_W^e	$\delta \sin^2\theta_W$
E158	0.026	50 GeV	~ 4 %	0.3 %
MOLLER	0.0056	11 GeV	~ 2.4 %	0.1 %

Experimental Considerations



$$\sqrt{s} = 4.5\ \mathrm{GeV}$$

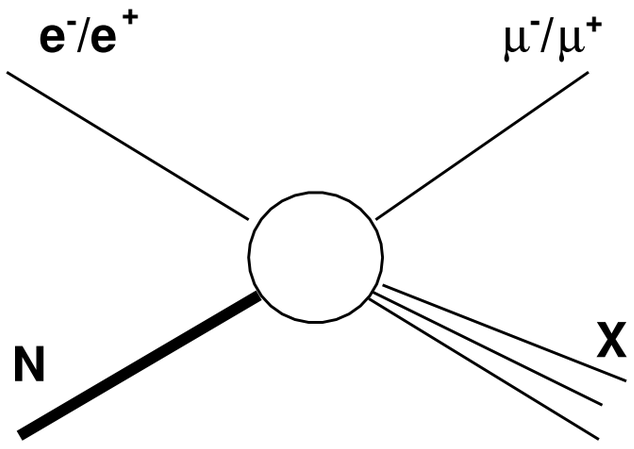
$$\mathscr{L} = 10^{36-39}\ \mathrm{cm}^{-2}\ s^{-1}$$

$$e^{\pm} + N \rightarrow \mu^{\pm} + X$$

- Required experimental capabilities:

-good muon detectors
-good charged particle tracking
-good vertex resolution

SoLID Experiment



$$\sqrt{s} = 4.5\ \mathrm{GeV}$$

$$\mathscr{L} = 10^{36-39}\ \mathrm{cm}^{-2}\ s^{-1}$$

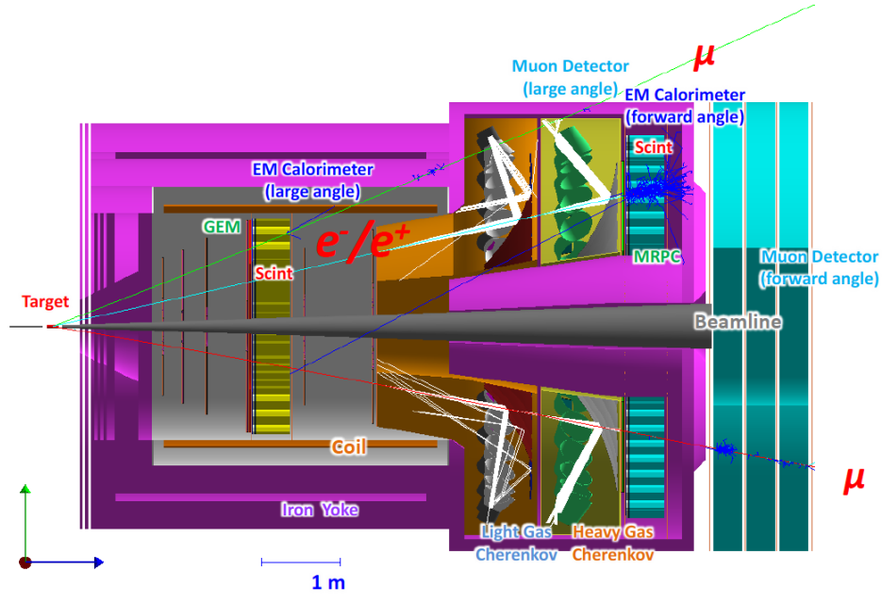


Fig. 3. The SoLID J/Ψ configuration with muon detectors [28]. Other sub-detectors are labeled.

$$e^{\pm} + N \rightarrow \mu^{\pm} + X$$

- Polar angle acceptance:

SIDIS configuration : $\theta = [8^{\circ}, 24^{\circ}]$

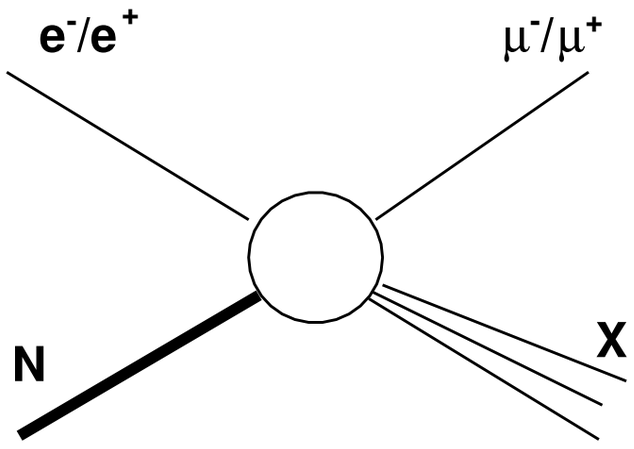
PVDIS configuration : $\theta = [22^{\circ}, 35^{\circ}]$

Most of the cross section is in the forward region due to the kinematic boost of a 11 GeV lepton beam.

- Azimuthal angle acceptance:

full-2π acceptance

SoLID Experiment



$$\sqrt{s} = 4.5\ \mathrm{GeV}$$

$$\mathscr{L} = 10^{36-39}\ \mathrm{cm}^{-2}\ s^{-1}$$

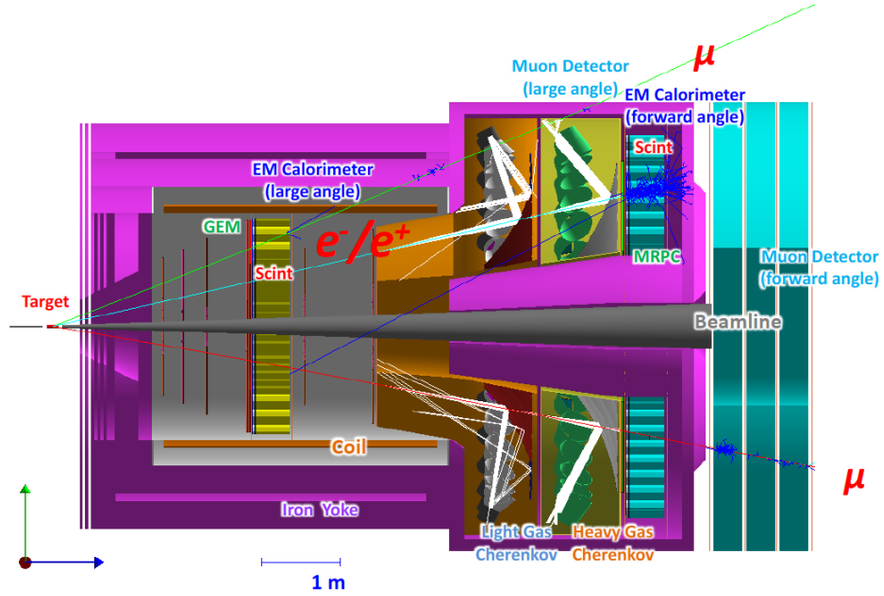


Fig. 3. The SoLID J/Ψ configuration with muon detectors [28]. Other sub-detectors are labeled.

$$e^{\pm} + N \rightarrow \mu^{\pm} + X$$

- Muon Chambers:

  The J/ψ and DDVCS configurations
  will be equipped with muon chambers

Muon Backgrounds

- The dominant background to the CLFV signal muon will come from decays of pions to muons:

$$\pi^+ \rightarrow \mu^+ \nu_\mu$$

- This background will be suppressed due to the compact size of of the SoLID detector, so that the typical pion decay length is much bigger than the distance to the detector from their production vertex.

$$P(L) = e^{-L/\lambda_D^\pi}, \qquad \lambda_D^\pi = \frac{p_\pi}{m_\pi c} c\tau.$$

- Pions will be typically produced with momenta in the range:

$$1\ \text{GeV} \lesssim p_\pi \lesssim 7\ \text{GeV}$$

- Thus, the typical pion decay lengths will be in the range:

$$56\ \text{m} \lesssim \lambda_D^\pi \lesssim 390\ \text{m} \qquad \gg \qquad \sim 5\ \text{m}$$

(Pion decay length)

(Overall detector dimensions, combined with proximity to pion production vertex)

- Correspondingly, the pion survival probability at the detector is:

$p_\pi \sim 1\ \text{GeV} \rightarrow 91\ \%$ survival probabilty
$p_\pi \sim 7\ \text{GeV} \rightarrow 99\ \%$ survival probabilty

Muon Backgrounds

- Charged particle tracking spatial resolution of 100 microns, allowing for precise reconstruction of pion decay vertices to further suppress backgrounds.

- Other backgrounds can arise from charmed meson decays or J/ψ decays. Once again tracking and vertex resolution capabilities can help suppress such backgrounds.

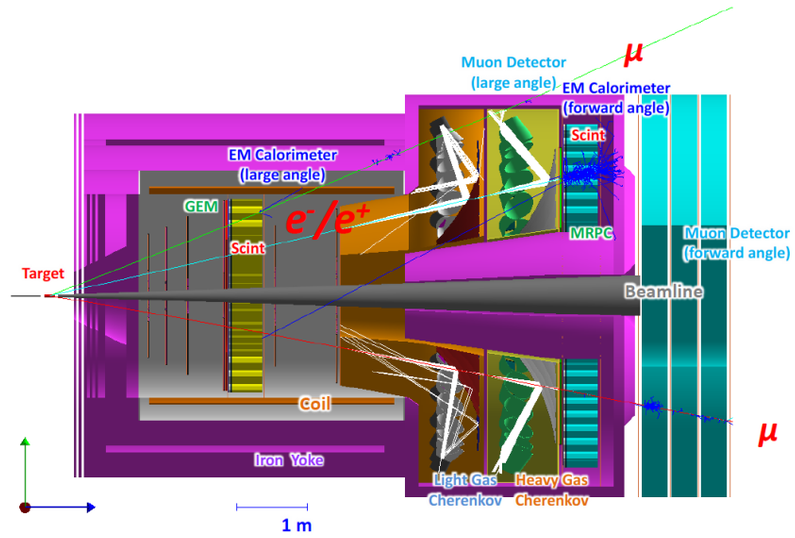


Fig. 3. The SoLID J/Ψ configuration with muon detectors [28]. Other sub-detectors are labeled.

- Due to the small center of mass energy, $\sqrt{s} \sim 4.5\ \mathrm{GeV}$, there are no backgrounds from B-meson decays.

More detailed simulation studies needed to estimate the impact of acceptance and backgrounds on CLFV limits.

Hadronic Effects

Corrections to Cahn-Gilman

- Hadronic effects appear as corrections to the Cahn-Gilman formula:

$$A_{RL} = -\frac{G_F Q^2}{2\sqrt{2}\pi\alpha}\frac{9}{10}\left[\tilde{a}_1 + \tilde{a}_2\frac{1-(1-y)^2}{1+(1-y)^2}\right]$$

$$\tilde{a}_j = -\frac{2}{3}(2C_{ju} - C_{jd})\left[1 + R_j(\text{new}) + R_j(\text{sea}) + R_j(\text{CSV}) + R_j(\text{TMC}) + R_j(\text{HT})\right]$$

New physics

Sea quarks

Charge symmetry violation

Target mass

Higher twist

- Hadronic effects must be well understood before any claim for evidence of new physics can be made.

[Bjorken, Wolfenstein; Hobbs, Melnitchouk;
SM, Ramsey-Musolf, Sacco;
Belitsky, Mashanov, Schafer;
Seng, Ramsey-Musolf, ….]

Some Definitions and Notation

- Asymmetry can be brought into the form:

$$A_{RL} = -\left(\frac{G_F Q^2}{4\sqrt{2}\pi\alpha}\right)\left[g_A^e Y_1 \frac{F_1^{\gamma Z}}{F_1^\gamma} + g_V^e Y_3 \frac{F_3^{\gamma Z}}{F_1^\gamma}\right]$$

- The Y_1 factor has the form:

$$Y_1 = \left(\frac{1+R^{\gamma Z}}{1+R^\gamma}\right)\frac{1+(1-y)^2 - y^2\left[1 - r^2/(1+R^{\gamma Z})\right] - 2xyM/E}{1+(1-y)^2 - y^2\left[1 - r^2/(1+R^{\gamma})\right] - 2xyM/E}$$

- The Y_3 factor has the form:

$$Y_3 = \left(\frac{r^2}{1+R^\gamma}\right)\frac{1-(1-y)^2}{1+(1-y)^2 - y^2\left[1 - r^2/(1+R^{\gamma})\right] - 2xyM/E}$$

- We have used the definitions:

$$R^{\gamma(\gamma Z)} \equiv \frac{\sigma_L^{\gamma(\gamma Z)}}{\sigma_T^{\gamma(\gamma Z)}} = r^2 \frac{F_2^{\gamma(\gamma Z)}}{2xF_1^{\gamma(\gamma Z)}} - 1, \qquad r^2 = 1 + \frac{4M^2x^2}{Q^2}$$

Key features of the Asymmetry Terms

- Asymmetry can be brought into the form:

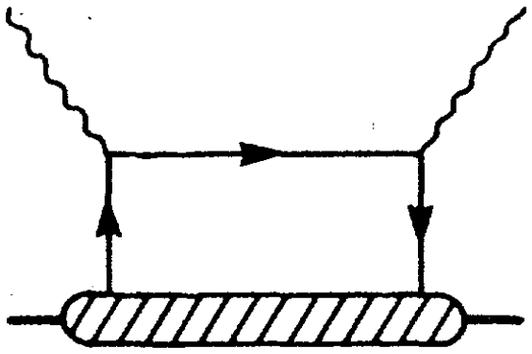
$$A_{RL} = -\left(\frac{G_F Q^2}{4\sqrt{2}\pi\alpha}\right)\left[g_A^e Y_1 \frac{F_1^{\gamma Z}}{F_1^\gamma} + g_V^e Y_3 \frac{F_3^{\gamma Z}}{F_1^\gamma}\right]$$

- Dominant term in asymmetry
- Can in principle be kinematically distinguished from second term (independent of y)
- Can be sensitive to only quark-quark correlations
- A single twist-4 matrix element determines quark-quark correlations.

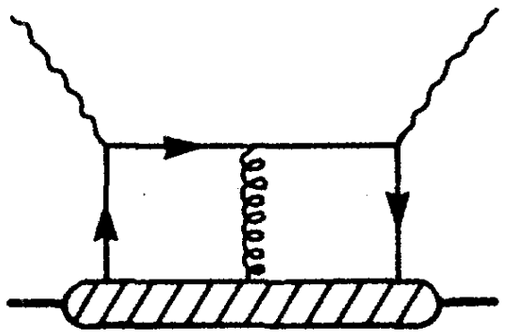
[Bjorken, Wolfenstein;
SM, Ramsey-Musolf, Sacco]

- suppressed by small electron vector coupling
- Can be kinematically distinguished from second term(dependent on y)
- Can be sensitive to quark-quark and quark-gluon correlations
- Multiple twist-4 matrix elements determine correlations
- Can be extracted from neutrino scattering data

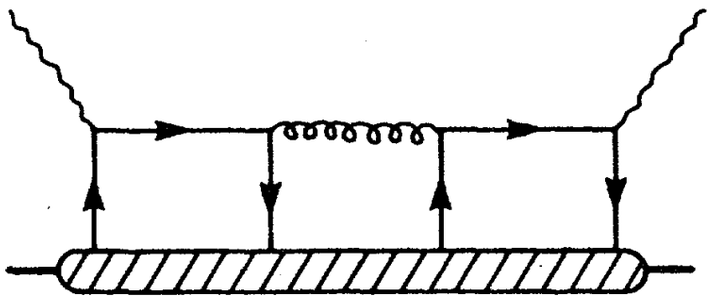
Operator Product Expansion



Twist-2



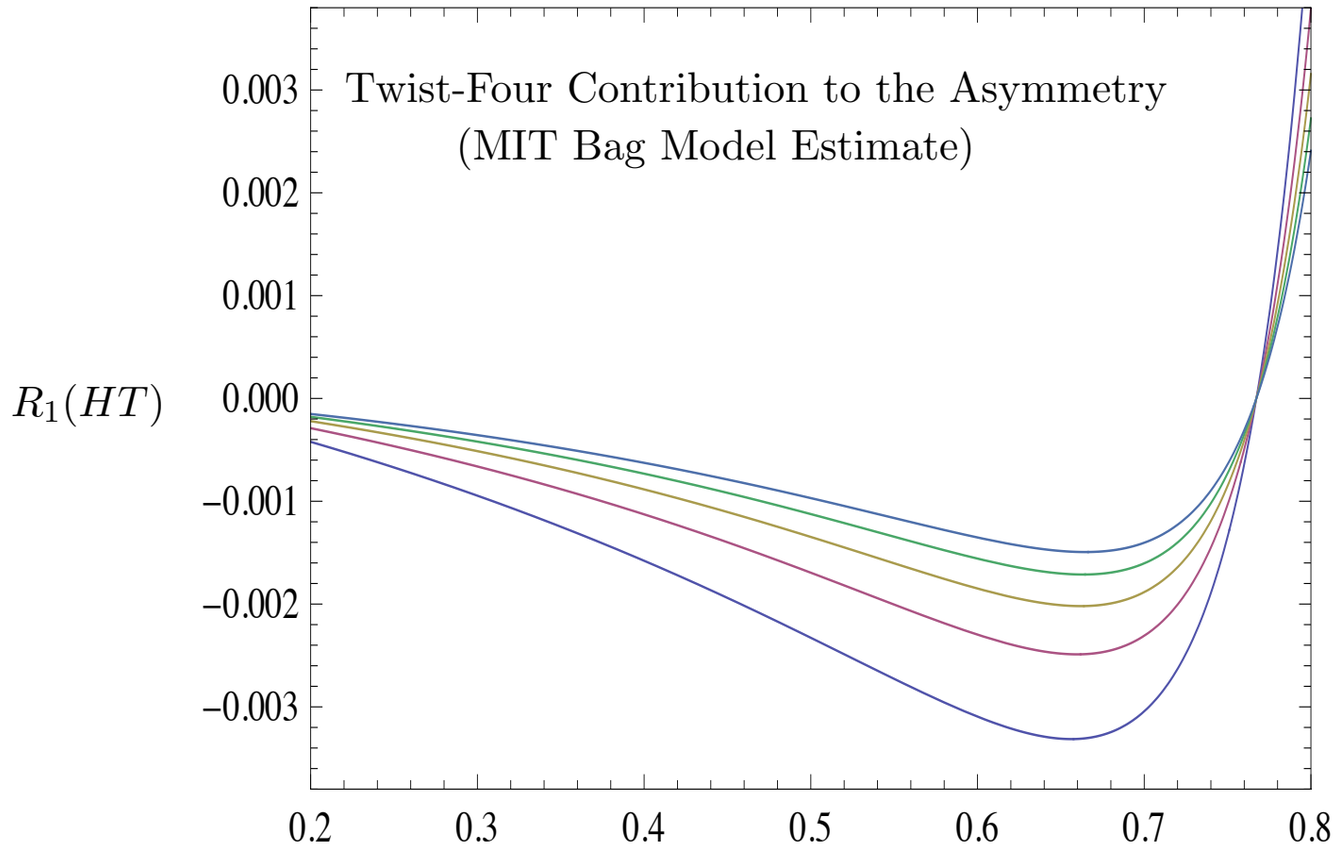
Quark-gluon correlation (Twist-2 + Twist-4)



Quark-quark correlation(Twist-4)

$$\mathcal{O}_{ud}^{\mu\nu}(x) = \frac{1}{2}[\bar{u}(x)\gamma^{\mu}u(x)d(0)\gamma^{\nu}d(0) + (u \leftrightarrow d)]$$

Form of twist-4 correction



[SM, Ramsey-Musolf, Sacco]

$$R_1(\mathrm{HT}) = \left[\frac{-4}{5(1-\frac{20}{9}\sin^2\theta_W)}\right]\frac{F_1^{du}}{u_p(x)+d_p(x)}.$$

- Bag model estimate of quark-quark correlation is below the half-percent level.

- If the Bag Model estimate is accurate, then higher twist effect is small and becomes difficult to extract.

Charge Symmetry Violation (CSV)

[Hobbs,Melnitchouk]

- Parameterization of CSV effects:

$$\begin{aligned} u_p &= u + \frac{\delta u}{2} \\ d_p &= d + \frac{\delta d}{2} \\ u_n &= d - \frac{\delta d}{2} \\ d_n &= u - \frac{\delta u}{2} \end{aligned} \quad \longrightarrow \quad R_1(\mathrm{CSV}) = \left[\frac{1}{2}\left(\frac{2C_{1u}+C_{1d}}{2C_{1u}-C_{1d}}\right) - \frac{3}{10}\right]\left(\frac{\delta u - \delta d}{u+d}\right)$$

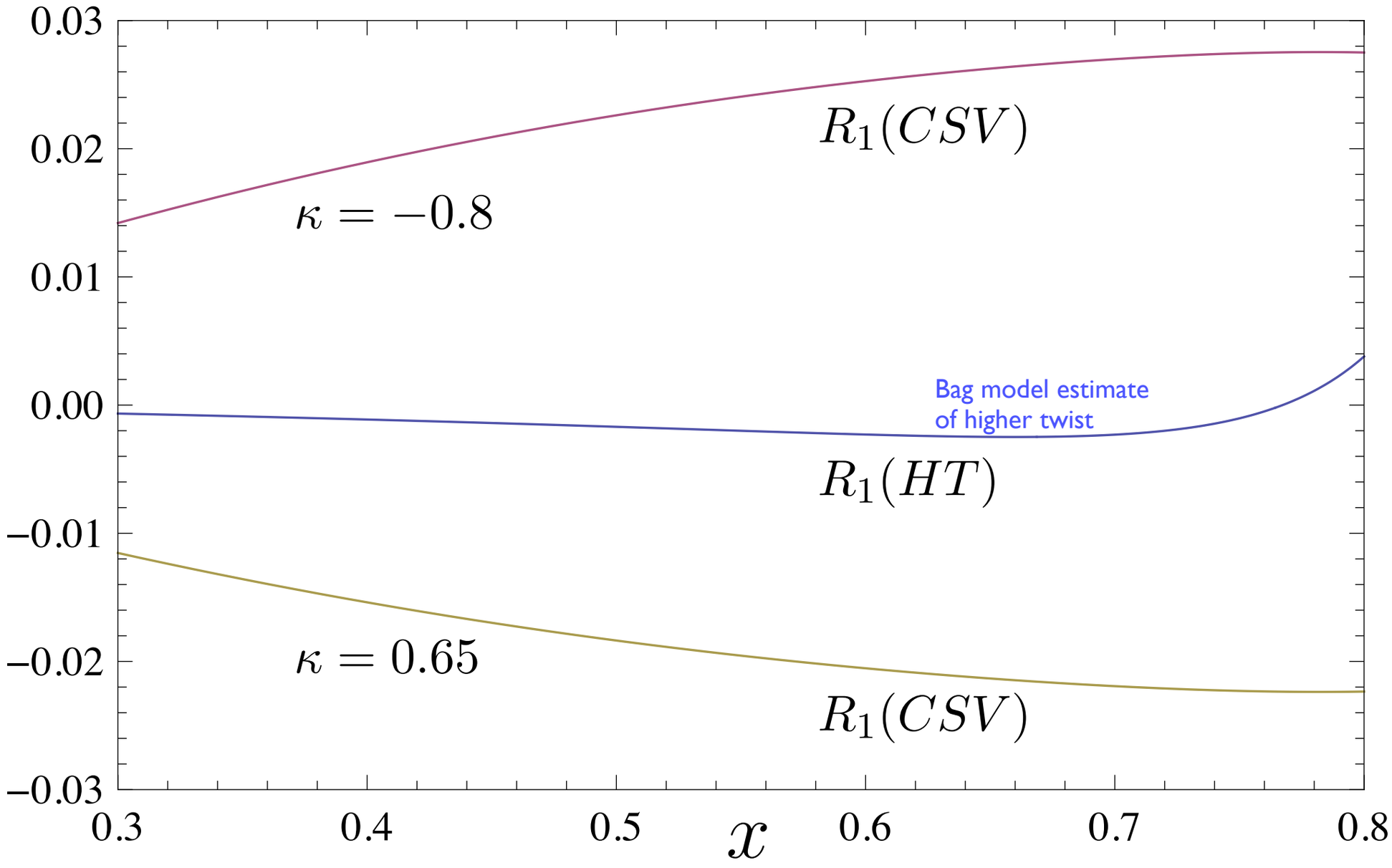
- Phenomenological model of CSV effects:

$$\delta u - \delta d = 2\kappa f(x)$$

$$f(x) = x^{-1/2}(1-x)^4(x-0.0909)$$

CSV vs Higher Twist

[SM, Ramsey-Musolf, Sacco]



- These estimates indicate that HT effects may be small compared to CSV effects.

SoLID Projection Analysis $\sin^2\theta_W$ Extraction

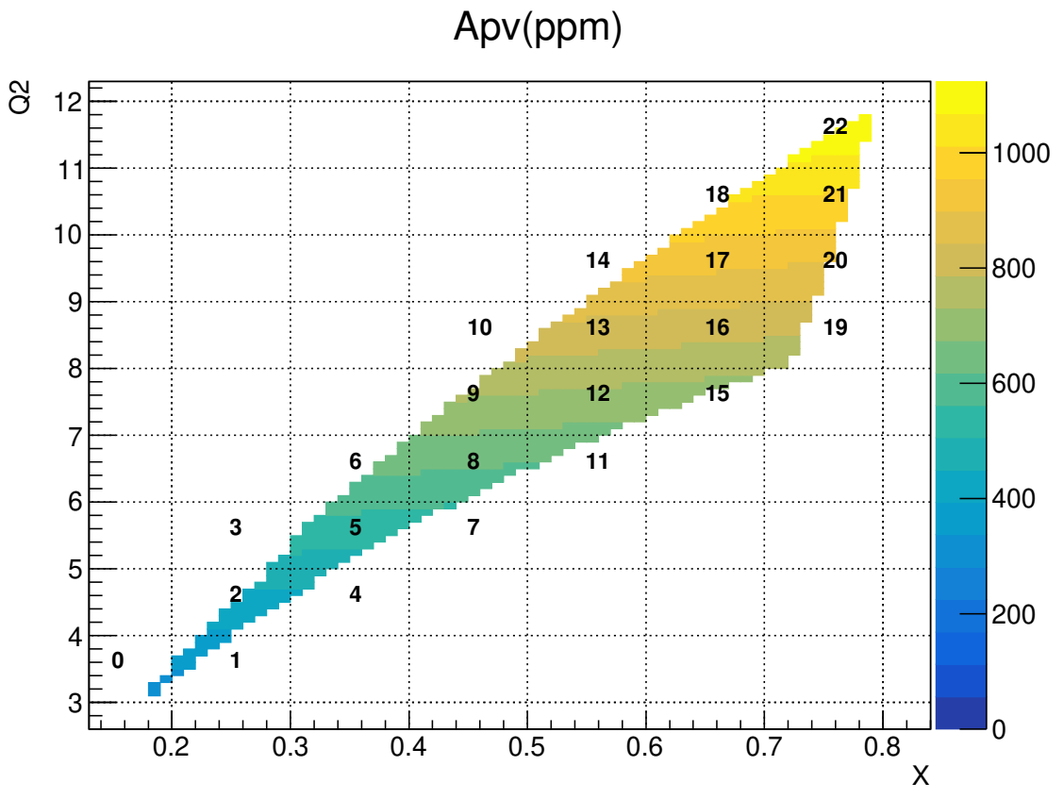


FIG. 11. Illustration of PVDIS asymmetry on a deuteron target in ppm on the (x, Q^2) plane. The data are divided into evenly spaced grid with the bin number shown. The expected statistical uncertainty is less than 1% in most of the bins.

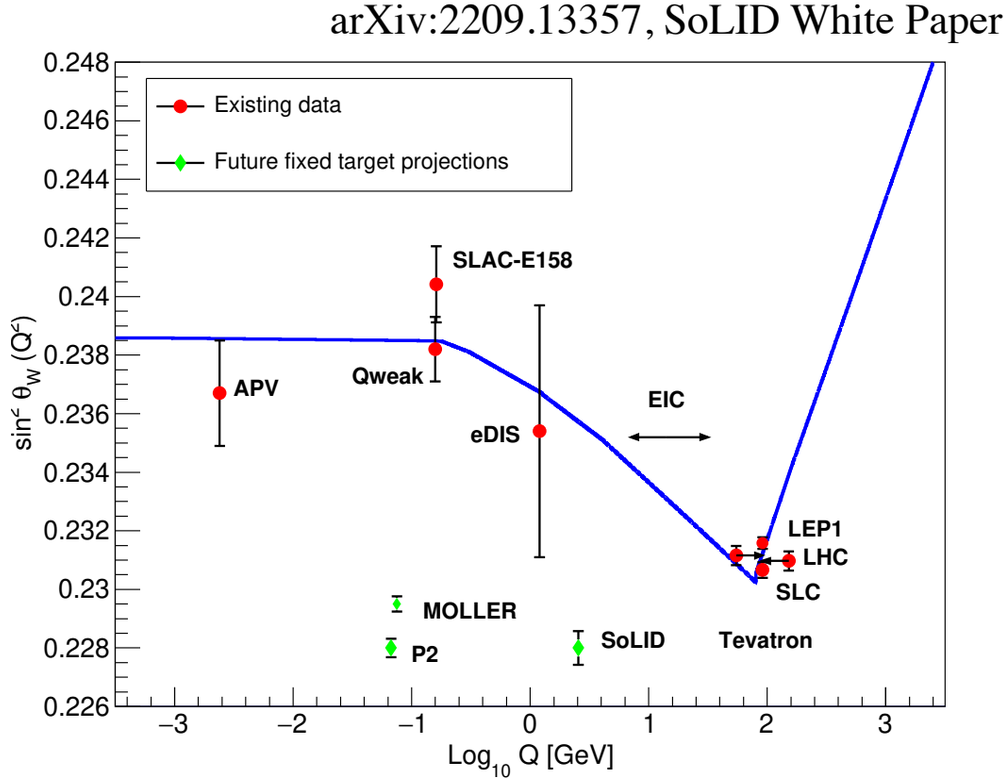


FIG. 12. Experimental determination of the weak mixing angle $\sin^2\theta_W$. Data points for Tevatron and LHC are shifted horizontally for clarity.

$$A_{PV}^{\mathrm{data}} = A_{PV,(d)}^{\mathrm{SM}}\left(1 + \frac{\beta_{\mathrm{HT}}}{(1-x)^3 Q^2} + \beta_{\mathrm{CSV}} x^2\right)$$

[Emmert, Nycz, Zheng]

Uncertainty Contributions to A_{PV}

- Statistical uncertainty

$$dA_{PV}^{\text{stat}} = \frac{1}{P_e\sqrt{n_b}} = \sigma_{\text{stat},b}$$

with $P_e = 0.8$ and bin event count n_b computed from rates for **120 days** of run time

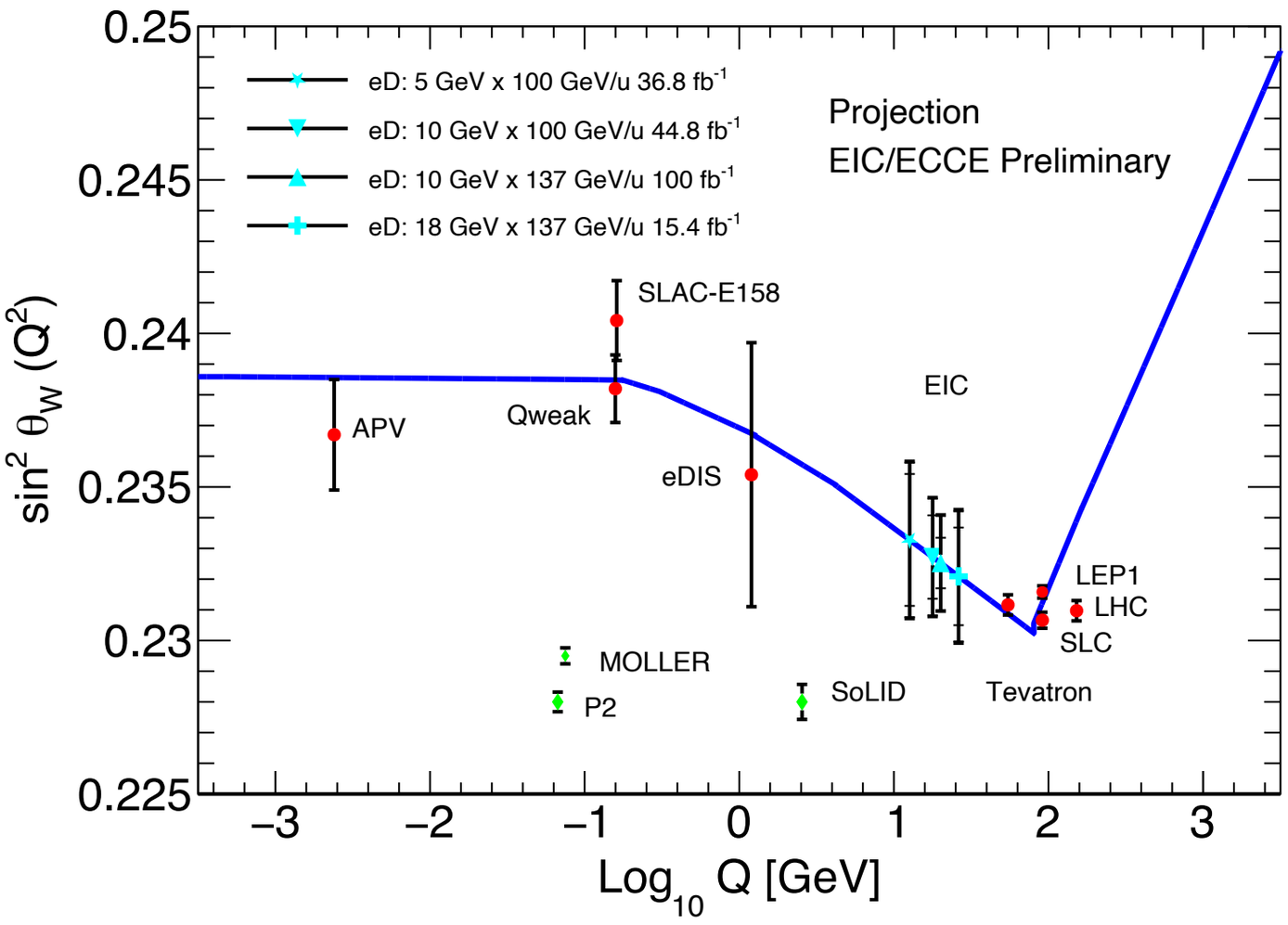
- Experimental systematic uncertainties

Source	Relative Uncertainty dA/A
Beam polarization	0.4%
Q^2 determination	0.2%
Event reconstruction	0.2%
Radiative correction	0.2%

Completely correlated ($\sigma_{\text{corr}}/A = 0.45\%$)

Uncorrelated ($\sigma_{\text{uncorr}}/A = 0.28\%$)

Extraction of the Weak Mixing Angle



[Boughezal, Emmert, Kutz, SM, Nycz, Petriello, Simsek, Wiegand, Zheng]

- SoLID can extract the weak mixing angle with higher precision than the EIC.

Extraction of d/u Ratio from PVDIS on

- PVDIS asymmetry with a proton target (ignoring sea quarks):

$$A_{RL}^{p} = \frac{3G_F Q^2}{2\sqrt{2}\pi\alpha} \frac{(2C_{1u} - d/u\, C_{1d}) + Y\,(2C_{2u} - d/u\, C_{2d})}{4 + d/u}$$

$$Y = \frac{1-(1-y)^2}{1+(1-y)^2}$$

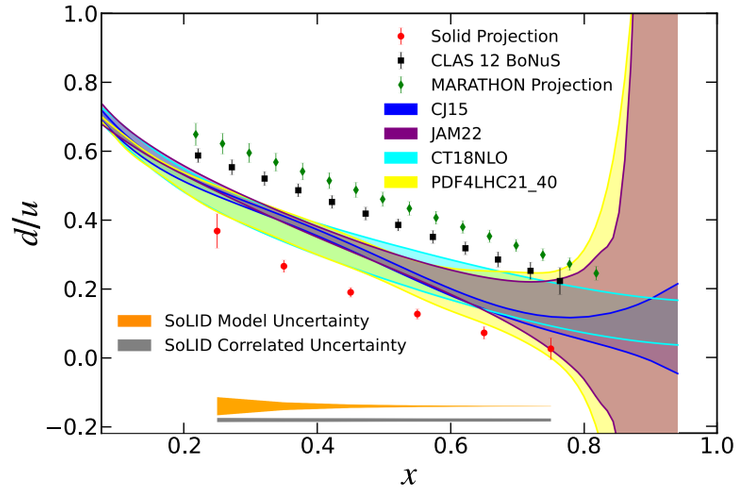


FIG. 14. Projected results on the PDF ratio d/u from the PVDIS proton measurement (red points) compared with the current world fits from a number of PDF groups and their uncertainties. The error bars of the SoLID projection indicate the uncertainty in the extracted d/u from statistical uncertainties, while uncorrelated systematic uncertainties are negligible. The two horizontal shaded bands show the uncertainty in d/u due to omitting sea quarks in Eq. (25) (model uncertainty, orange-colored band), and from correlated systematic uncertainties (dark grey band). Projections on MARATHON and CLAS12 BoNuS are from their respective experimental proposals [72, 73].

- Typically d/u is extracted from a comparison of fully inclusive DIS on proton vs deuteron targets. However, nuclear effects in the deuteron need to be modeled well to extract d/u.

- The PVDIS asymmetry allows for an extraction of proton PDF ratio d/u in the valence quark region, free of nuclear effects.

- Other complementary experiments (BoNuS, MARATHON) use different nuclear targets to extract d/u.